

AD-A260 181



ITATION PAGE

Form Approved
OMB No. 0704-0188

2

ed to average 1 hour per response, including the time for reviewing instructions, searching existing data sources, viewing the collection of information. Send comments regarding this burden estimate or any other aspect of this burden, to Washington Headquarters Services, Directorate for Information Operations and Reports, 1215 Jefferson Office of Management and Budget, Paperwork Reduction Project (0704-0188), Washington, DC 20503.

RT DATE

3. REPORT TYPE AND DATES COVERED

Final 1 June 91 to 31 May 92

4. TITLE AND SUBTITLE

Visible Chemical Lasers : reactions of metastable oxygene and the study of the red "Yoshida" reaction

5. FUNDING NUMBERS

AFOSR - 91 - 0235

6. AUTHOR(S)

Professor Roger BACIS

7. PERFORMING ORGANIZATION NAME(S) AND ADDRESS(ES)

Laboratoire de Spectrométrie Ionique et Moléculaire
(CNRS - UA 171) - Université Lyon I - Bât. 205
43, boulevard du 11 Novembre 1918
69622 Villeurbanne Cedex France

8. PERFORMING ORGANIZATION REPORT NUMBER

9. SPONSORING/MONITORING AGENCY NAME(S) AND ADDRESS(ES)

Monitoring/Sponsoring Agency : European Office of Aerospace Research and Development, Box 14, FPO NY 09510 - 0200

10. SPONSORING/MONITORING AGENCY REPORT NUMBER

11. SUPPLEMENTARY NOTES

12a. DISTRIBUTION/AVAILABILITY STATEMENT

Approved for public release ;
Distribution unlimited

DTIC
ELECTE
FEB 11 1993
S E D

12b. DISTRIBUTION CODE

13. ABSTRACT (Maximum 200 words)

During the period covered by the U.S. Air Force Grant we have identified the CuCl_2 molecule as responsible for the I.R. and strong red emission in the "Yoshida" reaction". The deep potential well of the CuCl_2 ground state favours population inversion in the two involved excited states ($^2\Delta_g$ and $^2\Pi_u$). The lifetime of the highest excited electronic state ($^2\Pi_u$) makes laser action unlikely at 700 nm. But the metastable $^2\Delta_g$ state could reasonably be expected to sustain a population inversion.

14. SUBJECT TERMS

Spectroscopy and kinetics of the reaction of CuCl_2 with metastable oxygen and search for a population inversion

15. NUMBER OF PAGES

3 + 54

16. PRICE CODE

17. SECURITY CLASSIFICATION OF REPORT

Unclassified

18. SECURITY CLASSIFICATION OF THIS PAGE

Unclassified

19. SECURITY CLASSIFICATION OF ABSTRACT

Unclassified

20. LIMITATION OF ABSTRACT

Scientific Report-Grant AFOSR-91-0235

Visible Chemical Lasers :reactions of metastable oxygen and the study of the red "Yoshida" reaction.

The object of this research includes the study of potential chemical lasers operating in the visible region of the spectrum. In the work related in this report, we examine the possibility of obtaining laser oscillation from the interaction of metastable oxygen [$O_2(^1\Delta_g)$] with heated metals which results in intense red and near infrared emission.

The work began in 1990 in our laboratory, in cooperation with the "Office National d'Etudes et de Recherches Aeronautiques", supported by French organisations (DRET, CNRS,...) and in 1991 received financial support from the Department of the Air Force, European Office of Aerospace Research and Development (Grant N° AFOSR -91-0235).

In order to present the current state of this research we give the results obtained since this project was undertaken. Our work has been published in 6 papers (1-6) given at the end of this report.

We became interested in this subject after reading papers by Yoshida et al (7-8). They reported a new visible laser in the red, first attributed to oxygen dimol emission, using a chemically pumped iodine laser system (8). They observed an extremely large augmentation of the "oxygen dimol emission" by the injection of iodine vapor downstream of the $O_2(^1\Delta_g)$ generator. A gain of 2,8 % was reported (7).

In our preliminary work we reproduced the Yoshida reaction using a high-power chemical generator with a maximum flow rate of 0.4 mol/s of chlorine (1). The red emission intensity increases by 5-6 orders of magnitude when the $O_2(^1\Delta_g)$ passes from 3×10^{15} to 20×10^{15} molecules . cm^{-3} . But in our experimental conditions we did not obtain laser oscillation. The nature of the emitter was not known and the mechanism of the reaction not understood, so we began to investigate this chemical system in more detail.

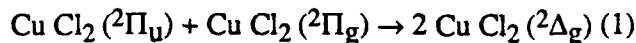
Preliminary spectra revealed that the presence of chlorine is necessary to obtain the red emission (2). The emitting species was identified later on as $CuCl_2$ (3).

The spectroscopy and electronic structure of $CuCl_2$ was poorly known and we have undertaken an extensive spectroscopic analysis of the electronic states of this molecule, together with a few attempts of lifetime measurements (4, 5, 6). At the present time the main results are the following.

The red emission is the ${}^2\Pi_u \rightarrow {}^2\Pi_g$ transition and the I.R. one is the ${}^1\Delta_g \rightarrow {}^2\Pi_g$ transition. The gas reaction zone is not very hot ($\sim 600\text{K}$) and the well depth of the ground state (${}^2\Pi_g$) is much greater than 5000 cm^{-1} . So numerous rovibrational levels of the ground state involved in the spontaneous emission from the lower ${}^2\Pi_u$ or ${}^1\Delta_g$ levels are not thermally populated. Then these excited levels have a population inversion with respect to a number of rovibrational levels of the ground state in the reaction.

Lifetime measurements made on the red ($\tau {}^2\Pi_u \leq 70\text{ ns}$) and IR ($\tau {}^1\Delta_g = 3.0 \pm 0.8\ \mu\text{s}$) systems match theoretical assignments of the electronic states of Cu Cl_2 (9) and fit also with the differences in intensity between the red (strong) and IR (weak) systems reported by Yoshida.

The ${}^2\Delta_g$ state is a reservoir state that can be populated by quasi-resonant process by O_2 (${}^1\Delta_g$) and also by energy exchange in collision between Cu Cl_2 (${}^2\Pi_u$) and Cu Cl_2 (${}^2\Pi_g$)



The question of using the chemical system as a laser was the main motivation for the study. Lifetime measurements in the red system of Cu Cl_2 and also efficient depopulation by the reaction (1) make laser action most unlikely at 700 nm. Indeed attempts to produce an optically C.W. pumped (Kr^+) Cu Cl_2 laser at 700 nm have failed.

But the metastable ${}^2\Delta_g$ state could reasonably be expected to sustain a population inversion with respect to the ground state of Cu Cl_2 provided that the population of this electronic state remain highly efficient.

Accession For	
NTIS CRA&I	<input checked="" type="checkbox"/>
DTIC TAB	<input type="checkbox"/>
Unannounced	<input type="checkbox"/>
Justification	
By	
Distribution/	
Availability Codes	
Dist	Avail and/or Special
A-1	

DTIC QUALITY INSPECTED 3

References

- 1) R. BACIS et al
Europhys. Lett. 12, 569 (1990)
Appendix 1
- 2) R. BACIS et al
8th International Symposium on Gas Flow and chemical Lasers, 10-14 September 1990
Madrid - SPIE Vol. 1397, 173 (1990)
Appendix 2
- 3) A.J. BOUVIER et al
J. de Physique IV , C7 , Vol. 1, 663 (1991)
Appendix 3
- 4) A.J. BOUVIER et al
Chem. Phys. Lett., 184, 133 (1991)
Appendix 4
- 5) A.J. ROSS et al
J. Mol. Spectrosc., to be published
Appendix 5
- 6) A.J. BOUVIER et al
9th International Symposium on Gas Flow and Chemical Lasers, 21-25 September 1992,
Heraklion, Crete, Greece - SPIE, to be published.
Appendix 6
- 7) S. YOSHIDA, M. TANIWAKI, T. SAWANO, K. SHIMIZU and T. FUJIOKA
Japanese J. of Appl. Phys. 28, L831 (1989)
- 8) S. YOSHIDA, K. SHIMIZU, T. SAWANO, T. TOKUDA and T. FUJIOKA
Appl. Phys.Lett. 54, 2400 (1989)
- 9) C.W. BAUSCHLICHER and B.O. ROSS
J. Chem. Phys. 91, 4785 (1989)

In this letter we report our preliminary investigations of the flame. Two types of experiments have been carried out. The first type is devoted to the spectroscopic analysis, using a medium-size chemical $O_2(^1\Delta_g)$ generator. The visible part of the emitted spectra as well as the infrared region have been recorded under various experimental conditions, with different metals placed in the metastable oxygen stream. The second type of experiments concerns the search of a laser effect, using a high-power chemical generator and copper which gives the brightest emission.

For the spectroscopic study, the experimental arrangement is very similar to the one described in ref. [1]. The chemical generator working at a flow rate of $(2 \div 3) \cdot 10^{-3}$ mol/s of chlorine delivers the same flow rate of oxygen, at a concentration of 60 to 80% in $O_2(^1\Delta_g)$, at a pressure of 0.7 to 1 Torr. After a water trap (liquid-nitrogen-cooled methanol $\approx -90^\circ C$), the O_2 flow reaches the reaction chamber, which is a rectangular duct 50 cm width and 2 cm in height. At mid-height, the O_2 flow crosses a stainless-steel tube of 4 mm external diameter which can be heated by an insulated resistor placed inside. Different metal wires (1 mm in diameter) can be wrapped around this tube. The emitted spectra are recorded in two ways: a Fourier transform spectrometer BOMEM DA3 for the visible range and a monochromator with a Ge detector for the infrared.

The effects of three metals have been investigated: copper, silver and aluminium. In each case, the red emission appears only above a certain metal temperature. For copper, this threshold seems to be around $200^\circ C$, while, for silver or aluminum, temperatures above $300^\circ C$ are required. Below these temperatures only the standard dimolar emission at 703 nm and 634 nm, the $O_2(^1\Sigma_g^+)$ emission at 762 nm and the $O_2(^1\Delta_g)$ emission at 1270 nm are observed. Above threshold, a completely different spectrum appears, as shown in fig. 1 and 2. Figure 1 gives the visible emission in the case of copper only. For silver or aluminum, the visible spectra obtained are almost the same as for copper, except that they are weaker in intensity by a factor of about 50. With the generator used for this study, which works at relatively low gas flow speeds, the red emission is seen around the metal surface and downstream. When the gas flow speed is increased, as in the second kind of experiments described below, the red emission can also be attached to the copper tube or can begin a few centimeters downstream after the metal contact, indicating a probable two-step reaction. Figure 2 gives the infrared spectra for copper and silver, with the $O_2(^1\Delta_g)$ emission observed

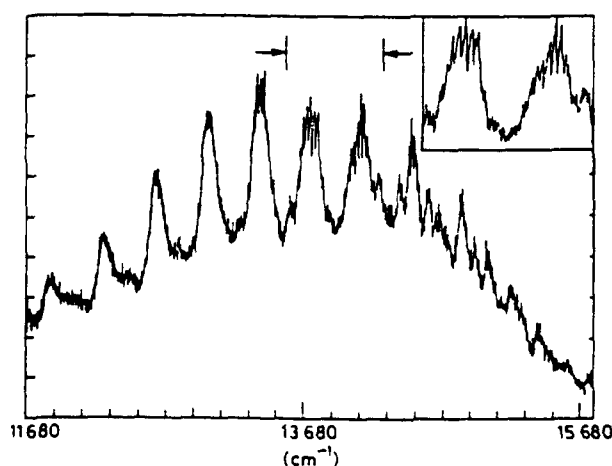


Fig. 1. - Visible emission spectrum (FT spectrometer: resolution 2 cm^{-1}). Copper rod ($300^\circ C$); oxygen flow rate $2.5 \cdot 10^{-3}$ mol/s. The insert corresponds to an enlarged portion of the spectrum as marked by arrows.

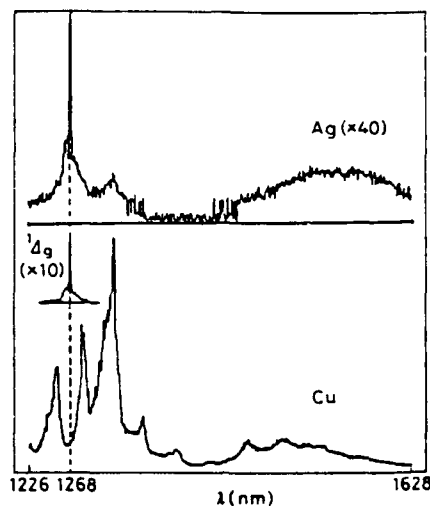


Fig. 2. - Infrared emission spectra (grating spectrometer: resolution 16 Å). Copper rod (300 °C); silver rod (550 °C); oxygen flow rate $3 \cdot 10^{-3}$ mol/s. The absence of the ${}^1\Delta_g$ peak in the Cu record denotes a strong consumption of $O_2({}^1\Delta_g)$. The vertical scales, in a.u., are the same for all spectra.

below threshold for comparison. Again the silver spectrum is weaker than for copper, but here the two spectra are not identical. The spectrum obtained using aluminum (not shown here) is similar to the silver spectrum. While for silver the $O_2({}^1\Delta_g)$ emission peak at 1270 nm remains, it vanishes in the presence of copper, where the total intensity of the infrared spectrum has been estimated to be about 250 times stronger than the $O_2({}^1\Delta_g)$ emission in the same conditions and below threshold. To our knowledge, these spectra do not appear in the reaction of metals with $O_2({}^3\Sigma_g^-)$ and are not due to excited usual metal oxide or chloride molecules. However, as the visible spectra are identical, we can attribute this emission to some oxygen complex, maybe excited states of O_3 or O_4 , while the infrared emission might reflect the interaction of $O_2({}^1\Delta_g)$ with the surface of the metal. Several facts lead us to think that the first step of the reaction is a metal oxide formation. In the case of copper, a black deposit, which analysis revealed to be a mixture of Cu_2O and CuO , is observed on the metal surface after a 20 minute run. On the walls of the cavity the deposit is brown, turning to white after a few minutes of atmospheric exposure. This second deposit could be copper hydroxide and chloride. But it should be stressed that only a small amount of metal is consumed in the reaction. For a 20 minute run giving about 3.5 moles of oxygen ($O_2({}^3\Sigma_g^-) + O_2({}^1\Delta_g)$), less than 0.5 g of copper oxides, «hydroxides» and «chlorides» is obtained. The quantity of deposit seems not to vary with pressure or gas flow speed ($(5 \div 15) \text{ m} \cdot \text{s}^{-1}$). Unfortunately, it was not possible to measure the consumption of $O_2({}^1\Delta_g)$ in the reaction.

A reaction step involving metal oxide formation could explain why the overall reaction is less efficient with Ag or Al than with Cu. The facts that only a tiny cavity wall deposit occurs for Ag and Al and that overheating the metal increases the red emission, much more in copper than for the other two, seem to confirm this hypothesis. However, it is not obvious that the copper oxide observed at the end of the experiment is due to the first reaction in the process. The infrared spectrum does not correspond to CuO and the visible spectra cannot be understood under this hypothesis. More likely, some copper peroxide CuO_n is primarily formed which dissociates into CuO and an excited oxygen complex via collisional processes.

The exact nature of this oxygen complex is not yet established. As shown in the inset of fig. 1, the broad peaks have a regular spacing of about 370 cm^{-1} , and each of them is structured by at least seven lines separated by 24 cm^{-1} . If Van der Waals molecules (O_2)₂ are to be considered, the 24 cm^{-1} spacing can be attributed to vibrational levels of the ground state ($^3\Sigma_g^- + ^3\Sigma_g^-$), as observed by Long and Ewing [3]. However, one could expect vibrational energy spacings in a Van der Waals bond to show a greater anharmonicity than is observed between the 7 peaks in our spectrum. But all the possible involved states ($^1\Delta_g + ^1\Delta_g$) or ($^3\Sigma_g^- + ^1\Sigma_g^+$) (involving local mode excitation in one of the O_2 units) observed [3] or predicted [4] would give rise to a band separation of roughly 1500 cm^{-1} , far removed from the observed spacing of 370 cm^{-1} . This energy difference corresponds to a ring puckering vibration, predicted in a theoretical study of cyclic O_4 [5]. But the corresponding excited state is predicted to lie about $30\,000\text{ cm}^{-1}$ above two oxygen molecules $\text{O}_2(^3\Sigma_g^-)$, i.e. much higher than the region observed in this work. The regular structure of the emission spectrum covering a large range ($10\,000 \div 17\,000\text{ cm}^{-1}$) is probably due to a small polyatomic molecule. Among various candidates, it is tempting to attribute the red emission to the $^1B_1 \rightarrow ^1A_1$ transition of the O_3 molecule. This would be the emission corresponding to the Chappius absorption band ([6] and references therein). Then the emission from 1B_1 would arrive at thermally unpopulated vibrational excited levels of 1A_1 , which would justify Yoshida's gain measurements. Unfortunately little is known on the vibrational structure of the involved levels. A reasonable vibrational assignment of the Chappius absorption band has been given by Levene *et al.* [7]. But from vibrational frequencies of 1A_1 [8] we cannot assign the regular ($360 \div 380\text{ cm}^{-1}$) progression in our recorded spectrum to the O_3 molecule.

So far, we have only discussed the polyatomic oxygen molecules. The flow also contains low concentrations of Cl_2 and H_2O . The role played by the halogen could be minor because at the end of each generator run, when the $\text{O}_2(^1\Delta_g)$ concentration in the flow is decreasing while the Cl_2 concentration increases, the intensity of the red emission always drops sharply. But the possible influence of Cl_2 cannot be ignored. In particular the cavity wall deposit is a complex compound containing O, Cl, Cu and H in proportions depending on the reaction conditions and it is possible that the polyatomic molecule formed in the second step is a chlorine derivative. It is also quite plausible that water, always present in the flow despite the cold trap, contributes to the process.

The overall spontaneous emitted powers in this experiment have been found to be of the same order for the visible and for the infrared, *viz.* a few tens of milliwatts in the copper case. Compared to the ($100 \div 150$) W available power carried by singlet oxygen, the emission yield is very low, and the visible emission spectrum covers a broad range of wavelengths. Under these conditions, it seems to be difficult to obtain visible laser oscillation with this set-up.

For this purpose, we have used a high-power chemical generator with a maximum flow rate of 0.4 mol/s of chlorine. The laser cavity consists of two maximum reflectivity concave mirrors of 5 m radius of curvature. Two sets of mirrors have been used. One set is centred at 740 nm , the other at 640 nm . The channel cross-section is $(150 \times 6)\text{ cm}^2$. A 120 cm long, 1.2 cm external diameter copper tube is placed across the flow in the midplane of the channel and parallel to the cavity axis at a distance of 5.4 or 17.5 cm for the 740 nm cavity and 17.5 cm only for the 640 nm cavity. The copper tube is heated between 220 and 240°C . Several runs have been carried out in a wide range of pressures (0.3 to 3.5 Torr) and chlorine flow rate ($7 \cdot 10^{-2}$ to $4 \cdot 10^{-1}\text{ mol/s}$) resulting in $\text{O}_2(^1\Delta_g)$ absolute concentrations varying from $3 \cdot 10^{15}$ to $2 \cdot 10^{16}\text{ molecules/cm}^3$. An intense red emission is observed downstream the copper tube and over its entire length, but so far no laser effect has been observed within the limited sensitivity of our photodetector, which is estimated to be of the order of 100 to $200\text{ }\mu\text{W}$.

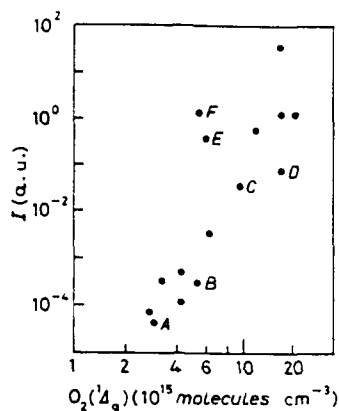


Fig. 3. - Intensity of the visible emission vs. $O_2(^1\Delta_g)$ concentration.

During these trials, the visible incoherent emission has been recorded with a silicon photodiode which was placed 17.5 cm downstream the copper tube. There are not enough experimental data to infer the effect of the various parameters independently. The emission intensity is given as a function of the $O_2(^1\Delta_g)$ concentration, which is the most sensitive parameter (fig. 3). The total intensity variation reaches six orders of magnitude but the measurement uncertainty is nearly one order of magnitude. This variation is very fast but we feel it is difficult to comment on this fact, since the experimental conditions were different from one point to the next. We have seen no correlation between the visible emission intensity and the total pressure. Water vapour is present in all experiments, yet we have seen no correlation between the visible emission and the partial pressure of water except for one set of experiments corresponding to points A, B, C and D of fig. 3. This set was collected with the water trap at room temperature. In this case the water pressure is much higher, of the order of 0.25 Torr. It can be seen that this excess does not prevent the visible emission but it tends to decrease its intensity. The effect of increasing the concentration of chlorine is not clear. A 4% excess of Cl_2 gives a much enhanced signal (point E) but increasing this excess to 40% (point F) gives no further improvement to within the accuracy of our intensity measurements.

A rough estimate of the spontaneous emitted power has been made. The highest intensity reported in fig. 3, taking into account geometrical factors, would correspond to at least a few watts for an active volume of about 15 litres. Compared with the small-scale experiment, the emitted power per unit volume is approximately ten times greater.

In conclusion, the previously reported laser effect [2] has not been reproduced in our experiments, in spite of the intense, uniform and extended active zone which is observed. Further developments of these preliminary studies are in progress in order to prove the potentiality of this system as a visible chemical laser.

Our spectroscopic study suggests that at least two steps have to be considered in the process. In the first one, the interaction of excited oxygen with the metal occurs, followed by a second step in which the reaction products interact with the remaining excited oxygen to produce the red emission. This innovative study of the effect of bringing an electronically excited molecule in contact with a metal surface presents some difficulties. Given the complexity of the spectra, which may arise from the formation of many possible species produced after the interaction of electronically excited species with metal surfaces, we have not yet managed to identify the emitting species. Further analysis is required for a complete

understanding of the observed phenomena, involving spectral analysis under higher resolution as well as mass spectrographic analysis of the species. It may also be that copper is not the best choice of metal for the oxygen complex formation, and a systematic investigation of the effects of other metals is in progress.

* * *

We thank Dr. S. YOSHIDA for interesting comments on this work, Dr. C. JOUVET for suggesting the possible existence of O_3 and D.R.E.T. (contracts 87/090, 89/34001).

REFERENCES

- [1] YOSHIDA S., TANIWAKI M., SAWANO T., SHIMIZU K. and FUJIOKA T., *Jpn. J. Appl. Phys.*, **28** (1989) L-831.
- [2] YOSHIDA S., SHIMIZU K., SAWANO T., TOKUDA T. and FUJIOKA T., *Appl. Phys. Lett.*, **54** (1989) 2400.
- [3] LONG C. A. and EWING G. E., *J. Chem. Phys.*, **58** (1973) 4824.
- [4] GOODMAN J. and BRUS L. E., *J. Chem. Phys.*, **67** (1977) 4398.
- [5] SEIDL E. T. and SCHAEFER III H. F., *J. Chem. Phys.*, **88** (1988) 7043.
- [6] GRIGGS M., *J. Chem. Phys.*, **49** (1968) 857.
- [7] LEVENE H. B., JONG-CHEN N. and VALENTINI J. J., *J. Chem. Phys.*, **87** (1987) 2583.
- [8] HERZBERG G., *Molecular Spectra and Molecular Structure III. Electronic Spectra and Electronic Structure of Polyatomic Molecules* (Van Nostrand Reinhold Company, New York, N.Y.) 1966.

APPENDIX 2

The new emission spectra from chemically excited oxygen and potentiality as a visible chemical laser.

R. Bacis*, J. Bonnet**, A.J. Bouvier*, S. Churassy*, P. Crozet*,
B. Erba*, E. Georges**, C. Jovet***, J. Lamarre**, Y. Louvet**, M. Nota*,
D. Pigache**, A.J. Ross* and M. Setra*

*Laboratoire de Spectrométrie Ionique et Moléculaire, Bâtiment 205,
43, boulevard du 11 novembre 1918, 69622 Villeurbanne CEDEX, France

** Office National d'Etudes et de Recherches Aérospatiales,
BP 72, 92322 Châtillon CEDEX, France

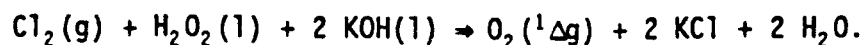
*** Laboratoire de Photophysique Moléculaire, Université Paris Sud
91405 Orsay CEDEX, France

ABSTRACT

The interaction of chemically generated metastable oxygen on various metals is examined. Spectra in the visible and the infrared are presented. A blue luminescence is seen for the first time. Small polyatomic molecules are probably responsible. An unsuccessful search for a laser effect has been made on a high power $O_2(^1\Delta_g)$ generator.

Recently Yoshida et al¹ have reported on an intense red emission which occurs when a high concentration flow of chemically produced metastable oxygen $O_2(^1\Delta_g)$ passes over heated copper (200-400°C). Laser gain at 703 nm¹ and laser oscillation at this wavelength of several tens of microwatts² have been reported by these authors. They suggested later on that the observed visible emission is due to stable oxygen dimer transitions and the possibility of a similar oxygen-dimer laser operating in the near infrared was also discussed.³ Stimulated by these results, we have undertaken various studies of what conditions affect the appearance and intensity of the red and infrared emission. We also have engaged a search for a laser effect. Preliminary results have just been published.⁴ In the present report, we summarize the main results obtained in Ref. 4, give a few details about some new observations and discuss hypotheses related to the mechanism of Yoshida's reaction.

A first series of spectroscopic analyses were performed on an experimental arrangement nearly similar to the one described in Ref. 1. The metastable oxygen $O_2(^1\Delta_g)$ is generated from the overall well known reaction:



Using concentrated H_2O_2 (85 %) and a small thickness of liquid (3-4 cm), we obtained a high concentration flow of $O_2(^1\Delta_g)$ (60-80 %), containing a certain amount of Cl_2 (a few percents).

The emitted spectra are recorded in two ways: a Fourier transform spectrometer BOMEM DA3 at 2 cm^{-1} resolution mainly for the visible range and a grating monochromator with a Ge or an MCT detector for the infrared.

The $\text{O}_2(^1\Delta_g)$ flow passes over a heated metal wire. The red emission appears only above a certain metal temperature (Cu: 200°C , Al: 300°C , Ag: 400°C). The visible emission extending from 10000 to 17000 cm^{-1} is almost the same with copper, aluminum or silver, but for aluminum and silver, its intensity is weaker by a factor of about 50. The visible spectrum shows two typical intervals between the peaks: $360\text{-}380\text{ cm}^{-1}$ and 25 cm^{-1} corresponding to different vibrational structures. The infrared emission extending from 6000 to 10000 cm^{-1} depends on the metal and the total emitted power is of the same order in the infrared and the visible.

Further, we observed a weak infrared emission when using copper. It is centered at 3200 cm^{-1} , red degraded, with 250 cm^{-1} full width at half maximum. We did not succeed in recording good spectra of the red emission at higher resolution. This seems mainly due to changes in the emission. That is a catalytic reaction beginning at the metal surface which is modified during the running time. We had to increase the metal temperature, then the gas temperature increases and the spectrum changes. We have shown in Ref. 4 that the red emission is not likely to be due to O_4 or O_3 and that the possible influence of Cl_2 or H_2O cannot be ignored. In particular, an excess of chlorine results in an enhancement of the red emission whereas an excess of water tends to quench it (see Fig. 3 - Ref. 4).

A chemical analysis of the deposits has shown that they were different on the copper rod (black deposit with formula close to $\text{Cu}_2\text{O}_{1.5}\text{Cl}_{0.5}$) and on the cavity walls. The latter is a white hygroscopic complex compound turning to green yellow in the presence of atmospheric air. It contains O, Cl, Cu and H in proportions depending on the reaction conditions ($\text{H}_x\text{Cu}_2\text{O}_{3.5}\text{Cl}_{4.5} - \text{H}_y\text{Cu}_2\text{O}_{2.5}\text{Cl}_4$).

After a vain search for a laser effect as explained below, we have determined that Yoshida's reaction can occur at low $\text{O}_2(^1\Delta_g)$ concentration and have set up an experiment where $\text{O}_2(^1\Delta_g)$ is obtained from a microwave discharge. In the meantime, we learned that Qi Zhuang et al⁵ had shown that the presence of Cl_2 was necessary to obtain the red emission. We have verified their results by introducing chlorine in the test cell of our microwave generator. A medium resolution spectrum has been obtained (2 cm^{-1} from a grating spectrometer). It is shown in figure 1 between 630 and 660 nm. The 25 cm^{-1} spacing structure observed for the first time in the 660-800 nm range with a chemical generator⁴ is also present in this wavelength range. Moreover, we obtained the same red emission when replacing Cl_2 by HCl . The spectrum is shown in figure 2. An intense $\text{O}_2(^1\Sigma_g^+) \rightarrow \text{O}_2(^3\Sigma_g^-)$ emission is observed because of the absence of water vapor which is an efficient quencher of $\text{O}_2(^1\Sigma_g^+)$. As little as 100 ppm of HCl are enough to generate a detectable emission. Although we did not take special care to eliminate water vapor traces, this shows that it is probable that the intense red emission is related to Cl_2 and not to H_2O or other H-compound. In another experiment we introduced water vapor instead of chlorine and observed no emission. We have also observed a blue luminescence at the closure of the chlorine flow. This luminescence is initiated at the surface of the heated copper rod; its lifetime and intensity are comparable to those of the red glow. It persists for a few minutes, decreasing slowly. The emitter is identified as CuCl with transitions from several levels (Fig. 3).

Other experiments using a chemical generator show that, at high pumping speed the red emission may begin a few centimeters downstream from the metal contact.⁴ Preliminary experiments with a short reaction cavity have shown that after the interaction with copper the red signal decreases regularly ($\tau_R = (5-10) \times 10^{-3}$ s) and the infrared signal passes through a maximum 6×10^{-3} s after metal contact and then decreases ($\tau_{IR} = (10-15) \times 10^{-3}$ s). Then the red signal decreases quicker than the infrared one and at least two steps have to be considered in the process. In the first one, the interaction of excited oxygen and Cl_2 with the metal occurs, followed by a second step in which the reaction products interact with the remaining excited oxygen and maybe Cl_2 to produce the red glow. This red emission in the gas phase corresponds probably to a three-body collisional process (see reference 3 and in the following sections the variation of the red signal as a function of $O_2(^1\Delta_g)$). The nature of the emitters is unknown; various diatomic molecules such as Cl_2 , ClO , $CuCl$, CuO have been eliminated. Their spectroscopic constants are known and synthetic spectra have been plotted and fail to reproduce the observed ones. Their related emissions do not cover exactly the good regions and the vibrational separations do not agree with the observations. The red emitter is surely a small polyatomic molecule. Different candidates such as HO_2 , Cl_2O , $ClOH$, symmetric ClO_2 can be eliminated. Among the three isomers of Cl_2O_2 some of the lower vibrational modes could be operating. One of the most serious candidates is the asymmetric ClO_2 ($Cl-O-O$). The infrared emitter is also probably a small polyatomic molecule (CuO_2 , $CuOCl$). We are setting new experiments in order to try to identify the involved species.

For a search of a laser effect, we have used a high power chemical generator. The laser cavity consists of two maximum reflectivity mirrors. Two sets of mirrors have been used. One set is centered at 740 nm, the other at 640 nm. The channel cross section is 150×6 cm². A 120 cm long, 1.2 cm external diameter heated copper tube is placed across the flow in the mid-plane of the channel. Several runs have been carried out in a wide range of pressure (0.3 to 3.5 Torr) and chlorine flow rates (7×10^{-2} to 4×10^{-1} moles/s) resulting in $O_2(^1\Delta_g)$ absolute concentrations varying from 3×10^{15} molecules/cm³ to 2×10^{16} molecules/cm³. An intense red emission is observed downstream of the copper tube and over its entire length but so far no laser effect has been observed within the limited sensitivity of our photodetector, estimated to be of the order of 100 to 200 μW . The visible emission intensity has been recorded with a silicon photodiode. The intensity variation with $O_2(^1\Delta_g)$ concentration reaches six decades when the concentration of $O_2(^1\Delta_g)$ increases from 3 to 20×10^{15} molecules/cm³. The highest intensity would correspond to at least a few watts of spontaneous emitted power for an active volume of about 15 liters. The analysis of the phenomena is in progress but the previously reported laser effect² has not been reproduced in our experiments in spite of the intense, uniform and extended active zone which is observed. However, the potentiality of this system as a visible chemical laser remains and further developments of these preliminary studies are currently in progress.

A very recent paper, just published by R.N. Zare and co-workers,⁶ confirms that the presence of chlorine is necessary to obtain the red emission.

REFERENCES

1. S. Yoshida, M. Taniwaki, T. Sawano, K. Shimizu and T. Fujioka, "Observation of high laser gain at 703 nm in a new chemical system", Japanese J. of Appl. Phys., 28, p. L831-L833, 1989.

APPENDIX 3

JOURNAL DE PHYSIQUE IV
Colloque C7, supplément au Journal de Physique III, Vol. 1, décembre 1991

C7-663

EMISSION SPECTRA FROM THE CHEMICAL REACTION OF HEATED Cu WITH METASTABLE OXYGEN AND Cl₂, COMPARISON WITH LASER INDUCED FLUORESCENCE AND ABSORPTION SPECTRA OF CuCl₂

A.J. BOUVIER, R. BACIS, J. BONNET*, S. CHURASSY, P. CROZET, B. ERBA, J.B. KOFFEND**,
J. LAMARRE*, M. LAMRINI, D. PIGACHE* and A.J. ROSS

*Laboratoire de Spectrométrie Ionique et Moléculaire, Bât. 205, Université Lyon I, 43 boulevard du
11 novembre 1918, F-69622 Villeurbanne cedex, France*

**Office National d'Etudes et de Recherches Aéronautiques, BP. 72, F-92322 Châtillon cedex, France*

***The Aerospace Corporation, Box 92957 Los Angeles, California 90009, USA*

Abstract

We present the results of a spectroscopic investigation of CuCl₂ vapour obtained from laser induced fluorescence recorded by Fourier transform spectrometry, and give preliminary spectroscopic constants for the ²Π_u and ²Π_g states of Cu³⁵Cl₂. Coupled with data obtained from absorption experiments on CuCl₂, this work brings us closer to understanding the mechanism of the reaction of copper with chlorine in the presence of singlet oxygen (¹Δ_g), which is accompanied by an intense red flame. This emission has been proposed as a possible candidate for the production of a visible or infrared chemical laser. We consider this question in view of lifetime measurements on the ²Π_u state of the CuCl₂ molecule, now accepted to be the emitting species, and also compare the infrared and visible spectra of CuCl₂ with the chemiluminescence recorded around 1.2 and 0.7 μm.

Introduction

Since it was discovered that the reaction of heated copper with Cl₂ in the presence of O₂ (¹Δ_g) produces a bright red flame, there has been interest in this system as a potential chemically pumped visible laser. The emitting species has been identified as the ²Π_u state of CuCl₂ /1/, and the red emission ascribed to the ²Π_u - ²Π_g transition. There were no high resolution experimental data available in the literature for CuCl₂, although high quality ab initio calculations have been performed recently which include both ligand field and spin orbit splittings in the electronic states of CuCl₂ derived from the Cu 3d atom /2/, so we set out to derive reliable spectroscopic constants for the low-lying electronic states with a view to refining this assignment, and to understanding the reaction mechanisms and reaction rates involved in the chemiluminescence.

Obtaining high resolution spectra of CuCl₂ proved difficult. We wanted to work at about 700 °C to guarantee a reasonable vapour pressure of CuCl₂, but the molecule tends to reduce to CuCl + 1/2 Cl₂ on heating - and CuCl is known to form a stable, cyclic trimer in the gas phase. Even when CuCl₂ is isolated, its spectrum is complicated by the presence of two isotopes of Cu and of Cl. Because both the absorption and the chemiluminescent emission spectra were too congested to allow us to attempt a full analysis, we studied gaseous CuCl₂ by laser induced fluorescence, recording the emission on a Fourier transform spectrometer. We could thus populate a single level of the excited state, and study a much simpler emission spectrum.

To discover whether or not CuCl_2 was likely to produce a chemical laser, we went on to measure the lifetime of the excited state involved in the laser induced fluorescence experiment. A priori, visible laser action seems unlikely, as it will be difficult to maintain a population inversion in the ground state of CuCl_2 , even though the lower level can be chosen to be a thermally unpopulated vibrational level. Although attempts to reproduce the reported /3/ laser oscillation at 700 nm have failed, there is still a second candidate for laser action: the infrared transition around 1.2 μm .

Experiment

We produced CuCl_2 for absorption, laser induced fluorescence and lifetime measurements in a sealed quartz cell, containing 10 mg CuCl_2 powder plus a few torr Cl_2 to drive the equilibrium $\text{CuCl}_2 \rightleftharpoons \text{CuCl} + 1/2 \text{Cl}_2$ to the left. The cell was maintained at 700°C. The absorption and laser induced fluorescence spectra were recorded on a Bomem Fourier transform spectrometer in the infrared (around 1.2 μm) on an InGaAs detector, and in the visible/near infrared on a silicon avalanche detector. Fluorescence was excited by a series of laser frequencies around 15500 cm^{-1} from a cw single mode DCM ring dye laser (Spectra Physics 380) and by the red lines of a Kr^+ laser. The radiative lifetime of the $^2\Pi_u$ state of CuCl_2 was measured by detecting the decay of fluorescence at 700 nm after excitation by a pulsed laser source. We excited CuCl_2 with DCM ($\lambda = 635 \text{ nm}$) pumped by a copper vapour laser (repetition rate 6 kHz) and found a lifetime of 90 ns for the $^2\Pi_u$ state.

To record the chemiluminescence associated with the reaction between heated copper and chlorine in the presence of $\text{O}_2(^1\Delta_g)$, we used a microwave discharge to produce $\text{O}_2(^1\Delta_g)$, which was mixed with Cl_2 and allowed to react with hot Cu metal, as an alternative to the cumbersome setup required to produce $\text{O}_2(^1\Delta_g)$ in a chemical reaction /4/. This arrangement yielded lower concentrations of $\text{O}_2(^1\Delta_g)$, and thus weaker emission, but produced stable emission for about 2 hours, which was far more satisfactory for the Fourier transform spectrometer than the shorter run times achieved with the chemical generator of $\text{O}_2(^1\Delta_g)$. Spectra were again recorded by Fourier transform spectrometry.

Results

The spectra we obtained are illustrated in figures (1) and (2). Figure 1 shows the visible / near infrared spectrum obtained a) in the chemical reaction, and b) a typical laser induced fluorescence spectrum. Curve b is a series of P,R doublets sitting on a continuous band. The simplicity of the discrete part of the spectrum suggests that the molecule is linear and that only one mode of vibration (symmetric stretch) is observed. Treating the molecule as though it were strictly linear, we ~~we~~ used a linear least squares fit of 160 lines (corresponding to transitions to 7 vibrational levels of the ground state) to obtain the following parameters (in cm^{-1}) for the $^2\Pi_g$ state of CuCl_2

$$\begin{array}{llll}
 Y_{00} = 0.0 & Y_{10} = 370.3464 & Y_{20} = - 0.48854 & Y_{30} = 0.1831 \times 10^{-2} \\
 Y_{01} = 0.058224 & Y_{11} = - 1.2407 \times 10^{-3} & Y_{21} = - 1.012 \times 10^{-5} & \\
 Y_{02} = - 8.9 \times 10^{-9} & Y_{12} = 6.9 \times 10^{-10} & &
 \end{array}$$

The standard deviation of the fit was 0.009 cm^{-1} .

For the ${}^2\Pi_u$ state we find :

$$\begin{array}{lll} T_v = 15731.7 \text{ cm}^{-1} & B_v = 0.05183 \text{ cm}^{-1} & D_v = 3.0 \times 10^{-9} \text{ cm}^{-1} \\ T_{v+1} = 16067.2 \text{ cm}^{-1} & B_{v+1} = 0.05175 \text{ cm}^{-1} & D_{v+1} = 4.0 \times 10^{-9} \text{ cm}^{-1} \end{array}$$

At present, we cannot specify which spin-orbit components of the ${}^2\Pi$ states are observed.

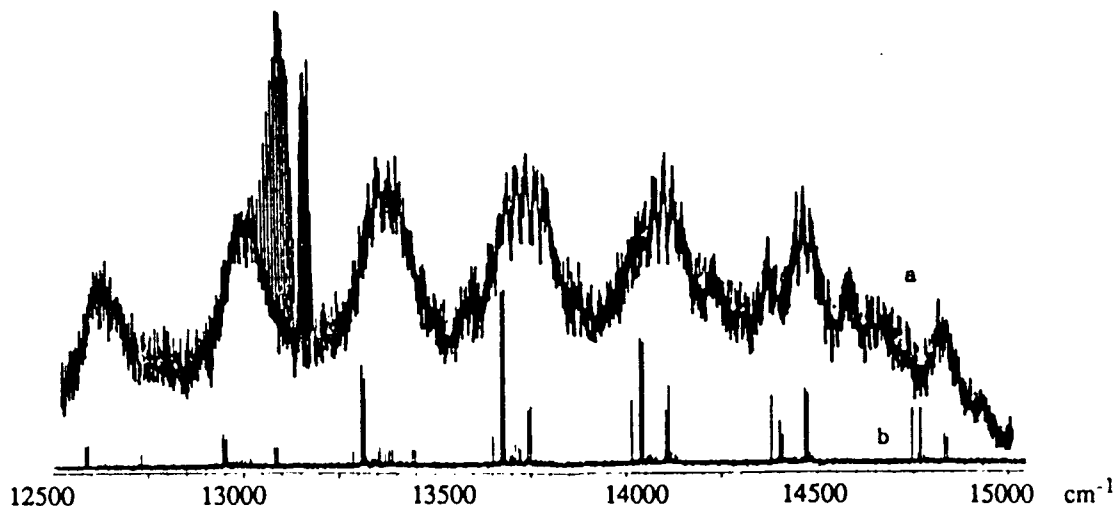


Figure 1 Visible / near infrared spectra.

- Chemiluminescence from the reaction $\text{Cu} + \text{Cl}_2 + \text{O}_2 ({}^1\Delta_g)$ at 350°C . Resolution = 0.25 cm^{-1} . The sharp bands at 13200 cm^{-1} correspond to $\text{O}_2 ({}^1\Delta_g \rightarrow {}^3\Sigma_g^-)$.
- Laser induced fluorescence. The laser gave 340 mW at 15502.06 cm^{-1} . The spectrum was recorded for 4 hours at a resolution of 0.08 cm^{-1} .

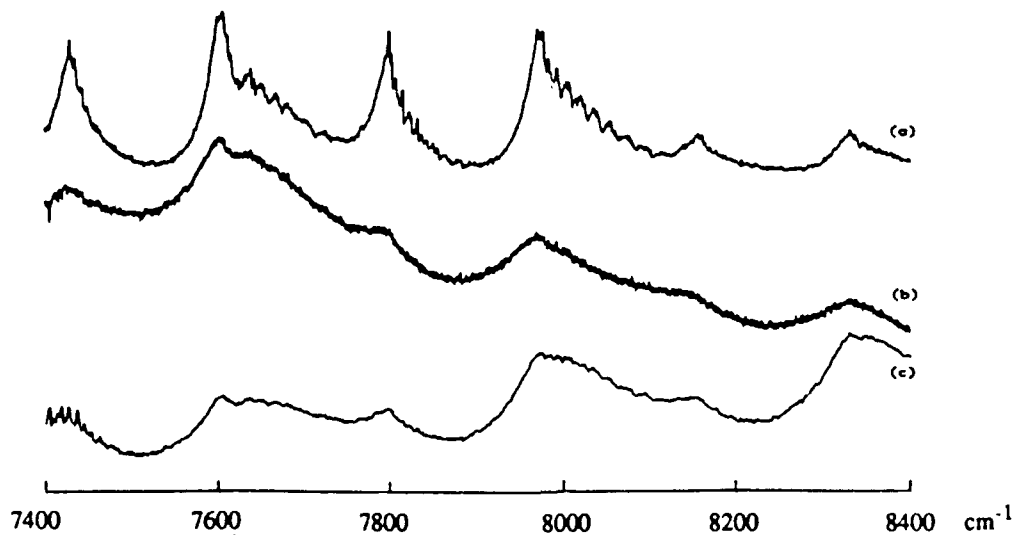


Figure 2 Infrared spectra, recorded at 0.5 cm^{-1} resolution.

- Chemiluminescence from the reaction $\text{Cu} + \text{Cl}_2 + \text{O}_2 ({}^1\Delta_g)$ at 350°C .
- Laser induced fluorescence, after subtraction of the blackbody contribution from the oven. This spectrum was totally insensitive to the choice of laser wavelength.
- The absorbance spectrum of CuCl_2 at 700°C ($\text{Log } I_0/I$ is = 0.02).

Discussion

The most striking feature is the similarity between the three IR spectra. Analysis of the laser induced fluorescence spectra revealed that the upper state was $^2\Pi_u$ - and we expected to see a similar discrete system, with P, Q and R branches in the infrared, corresponding to the $^2\Pi_u - ^2\Delta_g$ system (predicted by ab initio calculations to lie around 8000 cm^{-1}). Instead of this, we obtained a spectrum closely resembling the $^2\Delta_g - ^2\Pi_g$ system seen in absorption. At present, we suspect that the $^2\Pi_u$ state of CuCl_2 returns to the lower lying $^2\Delta_g$ state by a non-radiative process, perhaps by collision with CuCl_2 in the $^2\Pi_g$ state, or by predissociation followed by recombination of excited fragments. These processes explain the relatively short lifetime of the $^2\Pi_u$ state, (90 ns), and reduce the chances of being able to produce a chemical visible laser. This observation fits with several experimental failures to obtain laser action from the chemical reaction. However, it may be possible to produce laser action in CuCl_2 by optical pumping: investigations are in progress.

Conclusions

We have attributed the visible and infrared luminescence observed in the $\text{Cu} + \text{Cl}_2 + \text{O}_2 (^1\Delta_g)$ reaction to the $^2\Pi_u - ^2\Pi_g$ and $^2\Delta_g - ^2\Pi_g$ systems in CuCl_2 . We have used laser techniques in spectroscopy to obtain preliminary constants for the $^2\Pi_u$ and $^2\Pi_g$ states of $\text{Cu}^{35}\text{Cl}_2$, and to measure the lifetime of the $^2\Pi_u$ state. From our observations, we deduce that CuCl_2 is unlikely to become a visible chemically pumped laser.

References

- 1/ Tokuda, Y, Fujii, N., Yoshida, S., Shimizu, K. and Tanaka, I. Chem. Phys. Lett. 174 (1990) 385
- 2/ Bauschlicher, C.W. and Ross, B.O. J. Chem. Phys. 81 (1989) 4785
- 3/ Yoshida, S., Taniwaki, M., Sawano, T., and Shimizu, K. Jap. J. Appl. Phys. 28 (1989) L831
- 4/ Bachar, J. and Rosenwaks, S. Appl Phys. Lett. 41 (1982) 16

Comparison of emission spectra of CuCl_2 obtained via energy transfer from $\text{O}_2(^1\Delta_g)$ with laser-induced fluorescence spectra

A.J. Bouvier ^a, R. Bacis, J. Bonnet ^b, S. Churassy ^a, P. Crozet ^a, B. Erba ^a, J.B. Koffend ^c, J. Lamarre ^b, M. Lamrini ^a, D. Pigache ^b and A.J. Ross ^a

^a *Laboratoire de Spectrométrie Ionique et Moléculaire (associé au CNRS No. 171), Université Lyon I, Bâtiment 205,*

43 Boulevard du 11 Novembre 1918, 69622 Villeurbanne Cedex, France

^b *The Aerospace Corporation, Box 92957, Los Angeles, CA 90009, USA*

^c *Office National d'Etudes et de Recherches Aéronautiques, BP 72, 92322 Châtillon Cedex, France*

Received 22 March 1991; in final form 13 June 1991

Red and infrared ($\approx 8000 \text{ cm}^{-1}$) emission was recorded from a flame produced by Cl_2 and $\text{O}_2(^1\Delta_g)$ in the presence of hot copper, and from CuCl_2 excited directly by $\text{O}_2(^1\Delta_g)$. We note similarities between these spectra and an infrared absorption spectrum of CuCl_2 . Laser-induced fluorescence spectra of $\text{CuCl}_2(^2\Pi_u - ^2\Pi_g)$ were excited using the red lines of a krypton-ion laser, and recorded at high resolution on a Fourier-transform spectrometer. A preliminary analysis of the series of rotational doublets observed gives $T_e \approx 15800 \text{ cm}^{-1}$ for the $^2\Pi_u$ state and a well depth for $^2\Pi_g$ greater than 4300 cm^{-1} .

1. Introduction

Yoshida et al. [1] have reported an intense red emission that occurs when metastable oxygen, $\text{O}_2(^1\Delta_g)$, is passed over heated Cu metal. Gain at 700 nm [1] has been measured and laser oscillation at levels of several tens of microwatts have been announced [2] by these authors. They originally suggested that the emission was due to transitions in a stable oxygen dimer $(\text{O}_2)_2$ and the possibility of emission in the infrared was also discussed [3]. Stimulated by these results, several groups have investigated this system and several assignments of the carrier of this emission have been put forth [4–9]. Recently, Tokuda et al. [10] observed the same emission from CuCl_2 excited by $\text{O}_2(^1\Delta_g)$ and they have identified the carrier as CuCl_2 .

Currently, the spectroscopy and electronic structure of CuCl_2 are rather poorly known, especially with respect to its excited electronic states. Several low-resolution gas-phase absorption studies have been performed [11–14]. A broad continuous feature, peaking near 18000 cm^{-1} , is observed to dominate the visible region. A much less-intense system with

diffuse structure has been observed in the infrared near 8000 cm^{-1} . However, extinction coefficients reported in these investigations should be reconsidered in light of the subsequent work by Dienstbach et al. [15] where the dimerization of CuCl_2 to produce Cu_2Cl_4 was studied. They observed two totally symmetric Raman active modes indicating that CuCl_2 is not strictly a linear molecule, at least at elevated temperatures. Recent ab initio calculations [16] are in good agreement with experiment and predict a $^2\Pi_g$ ground state for CuCl_2 . An energy-level diagram of CuCl_2 is displayed in fig. 1.

2. Experiment

We modified our experimental apparatus [4] so that longer, stable running times are possible with our small chemical $\text{O}_2(^1\Delta_g)$ generator. The surface area of the copper was increased and the excited O_2 flow was confined to a $10 \times 10 \text{ cm}^2$ area in order to concentrate the flame to a smaller volume. Despite the intense red flame obtained using this apparatus, we were unable to record spectra at a resolution bet-

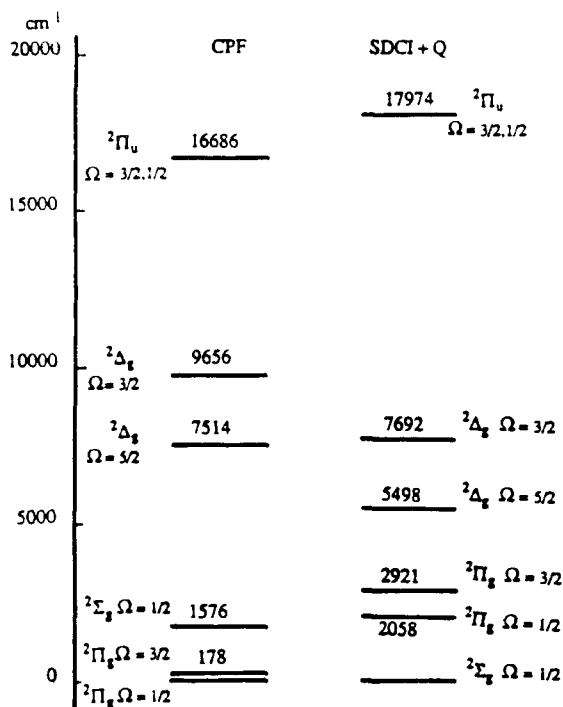


Fig. 1. Low-lying energy levels of CuCl_2 (from ab initio single and double CI and from coupled-pair functional calculations, ref. [16]).

ter than 2 cm^{-1} , due to fluctuations in the emission intensity caused by turbulence in the O_2 flow. It should be noted that the solid product that collected on the walls during the experiment was soluble in water and corresponds to CuCl_2 .

A new apparatus was constructed where the chemical $\text{O}_2(^1\Delta_g)$ source was replaced by a microwave discharge. This arrangement provided virtually unlimited running times, although at much reduced $\text{O}_2(^1\Delta_g)$ densities. Much more stable operation was obtained and all of the chemiluminescent emission reported here was recorded using this system. In addition, the copper-metal surface in this apparatus was interchangeable with a resistively heated stainless-steel crucible which was used for $\text{CuCl}_2/\text{O}_2(^1\Delta_g)$ studies. The anhydrous CuCl_2 , whose purity was 99.9% as stated by the manufacturer, was used without further purification.

Absorption and laser-induced fluorescence of CuCl_2 were performed using all-quartz cells. The 2.5

cm diameter cells have optically contacted Brewster-angle windows and 0.4 diameter sidearms for connection to the vacuum system, where sealing is done using a CH_4/O_2 torch, thus also fixing the vapour pressure while overheating the cell. The cells were flamed while containing 20–30 Torr Cl_2 , pumped out to less than 10^{-5} Torr, and then filled with several hundred milligrams of CuCl_2 and pumped again. 0.25 Torr Cl_2 was added to suppress decomposition of CuCl_2 into CuCl and Cl_2 . Part of the cell was immersed in liquid nitrogen to condense the Cl_2 gas and prevent its reaction with hot quartz while the cell was sealed. Spectra were recorded on a Bomem model DA 3 Fourier-transform spectrometer.

3. Results

Fig. 2 contains an infrared emission spectrum of the $\text{O}_2(^1\Delta_g)/\text{Cl}_2/\text{Cu}$ copper flame recorded at 1.0 cm^{-1} resolution using $\text{O}_2(^1\Delta_g)$ produced in a microwave discharge. The absorption spectrum of CuCl_2 in the same region taken through a 10 cm path-length quartz cell heated to 600°C is shown in fig. 3. The sidearm was maintained at 600°C while this spectrum was recorded. Both spectra can be considered to consist of two distinct series of bands. It is striking that the spacing between the features in both the emission (fig. 2) and the absorption (fig. 3) spectra

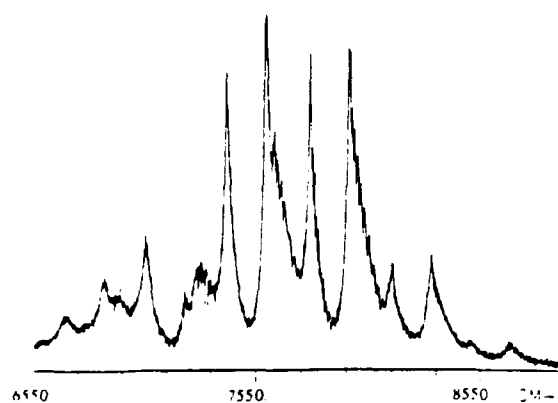


Fig. 2. Emission in the IR of the Yoshida flame. Resolution: 1 cm^{-1} ; recording time: 9 min. O_2 pressure: 1.04 Torr. $\text{O}_2(^1\Delta_g)$ from microwave generator; Cl_2 pressure: 0.25 Torr; copper temperature: 360°C .

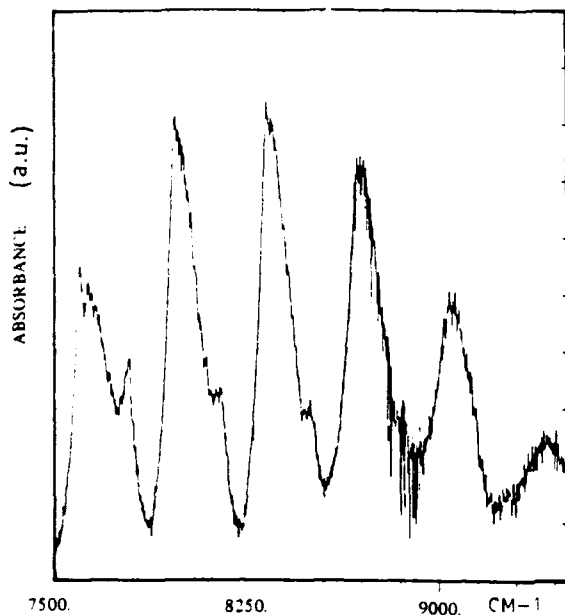


Fig. 3. Absorbance of the CuCl_2 molecule. Temperature of the cell: 600°C ; resolution: 2 cm^{-1} ; Cl_2 pressure: 0.2 Torr; length of the cell: 10 cm.

are very close, as indicated in table 1. The spacing between the broader bands in the emission spectrum and the main peaks in the absorption spectrum is 364 cm^{-1} and can be attributed to the CuCl_2 ground-state symmetric stretching mode. Previous workers [13,15] have reported values for ν_1 of 357 and $360 \pm 15\text{ cm}^{-1}$, while the ab initio [16] value is 373 cm^{-1} . The partially resolved shoulders visible in the absorption spectrum and the narrower bands in the emission spectrum also exhibit a spacing of 364 cm^{-1} . Depending upon how one performs the calculation, the separation between the two series in the emission spectrum is 177, 187, 541 or 551 cm^{-1} . None of these values lies close enough to reported frequencies for the anti-symmetric stretch [12,15] (496 ± 20 and 499 cm^{-1}) or the bending mode [15] (127 cm^{-1}) to warrant an assignment to either ν_2 or ν_3 . However, Bauschlicher and Ross [16] have calculated the CuCl_2 $^2\Pi_g$ ground-state spin-orbit splitting to be 178 cm^{-1} , suggesting that the two series correspond to transitions involving the $^2\Pi_g$ ($\Omega=1/2$) and $^2\Pi_g$ ($\Omega=3/2$) states. The use of the total electronic angular momentum Ω supposes that the molecule is linear and we neglect the vibrational angular momentum.

Table 1
Absorption and emission peaks in the CuCl_2 infrared spectrum

Absorption (cm^{-1})		Emission (cm^{-1})	
main peaks	shoulder	large peaks	narrower peaks
			6691.5
		6873.1	(181.6) (185.8)
		(water)	7058.9
			7428.3
7602		7603	(174.7) (195.5)
	7797		(173.5)
7970		7972	(183)
	(8150)		(176)
8330		8331	(181)
	(8508)		(181)
8700		8693	
9056			
9420			
average separation (cm^{-1})			
364	356	364	(177), (186)
			364

A portion of both the emission and absorption spectra at higher resolution is revealed in fig. 4. Under this resolution, small sub-bands are apparent in both spectra. The spacing between these sub-bands increases from 10 to 20 cm^{-1} in the broader bands of the emission spectrum while a constant spacing of 6–8 cm^{-1} is observed in the narrower bands. A similar trend is seen in the CuCl_2 absorption spectrum. These sub-bands probably arise due to differences in the bending-mode frequency in the two electronic states involved in the transition. However, more information is required for a definite assignment.

These considerations indicate that the infrared emission of the $\text{O}_2(^1\Delta_g)/\text{Cl}_2/\text{Cu}$ flame corresponds to the same transition as in the infrared absorption of the CuCl_2 molecule. The *ab initio* calculations of ref. [16] give the ground state of CuCl_2 as $^2\Pi_g$, and the only electronic state lying in the 7000–9000 cm^{-1} region is the $^2\Delta_g$ state. However, we cannot categorically state whether the $^2\Delta_g$ ($\Omega=3/2$) or $^2\Delta_g$ ($\Omega=5/2$) spin-orbit component, or both, are involved; this problem is raised below in section 4. It is worth

mentioning that the $g \leftrightarrow g$ symmetry rule will not be strict if the upper state is not linear, or if bending modes are excited.

We observed the CuCl_2 absorption spectrum in the visible region to have no structure, even at our highest resolution of 1 cm^{-1} . The absorption peak was determined to occur at $17900 \pm 100 \text{ cm}^{-1}$, in a cell at 600°C. The peak absorption in the visible is about 15 times stronger than that in the infrared range. Previous reports of the position of the absorption maximum range from 17950 [15] to 19000 [13] cm^{-1} . The disparity among these values probably stems from the $\text{CuCl}_2 \rightleftharpoons \text{Cu}_2\text{Cl}_4$ equilibrium [15] which was not always taken into account. The CuCl_2 absorption peaks near 17250 cm^{-1} while the dimer spectra peak at shorter wavelengths near 20000 cm^{-1} .

We also investigated the red emission from direct excitation of CuCl_2 by $\text{O}_2(^1\Delta_g)$, for comparison with the red emission Yoshida et al. [1] first observed with the $\text{O}_2(^1\Delta_g)/\text{Cl}_2/\text{Cu}$ system. Anhydrous CuCl_2 was placed in the stainless-steel crucible and $\text{O}_2(^1\Delta_g)$, produced in a microwave discharge, was slowly flowed over it. A red flame was observed whose maximum emission intensity occurred at a crucible temperature of 370°C, corresponding to the melting point of the CuCl_2 crystals. We then replaced the crucible and CuCl_2 by a heated Cu ring, introduced some Cl_2 into the $\text{O}_2(^1\Delta_g)$ flow and obtained red emission, stronger than that obtained using CuCl_2 . However, the spectrum of this emission was the same as that observed using the $\text{CuCl}_2/\text{O}_2(^1\Delta_g)$ alone. Several species are created by heating anhydrous CuCl_2 under our experimental conditions. These include [15] Cl_2 , CuCl , CuCl_2 , and Cu_2Cl_4 , among others. A possible explanation for the weaker emission intensity in the CuCl_2 case is that the dominant species is probably [15] Cu_2Cl_4 , which must be dissociated into CuCl_2 by $\text{O}_2(^1\Delta_g)$ collisions before emission can take place.

To provide more evidence that CuCl_2 indeed is the carrier of the emission observed in the $\text{O}_2(^1\Delta_g)/\text{Cl}_2/\text{Cu}$ system, we investigated the laser-induced fluorescence (LIF) of this molecule. The quartz cell containing CuCl_2 and a small amount of Cl_2 was heated in an oven to 600°C while the sidearm was maintained at 350°C. The two red lines, 676.4 and 647.1 nm, of a Kr^+ laser were used to excite the fluorescence. We note that the LIF intensity was dependent

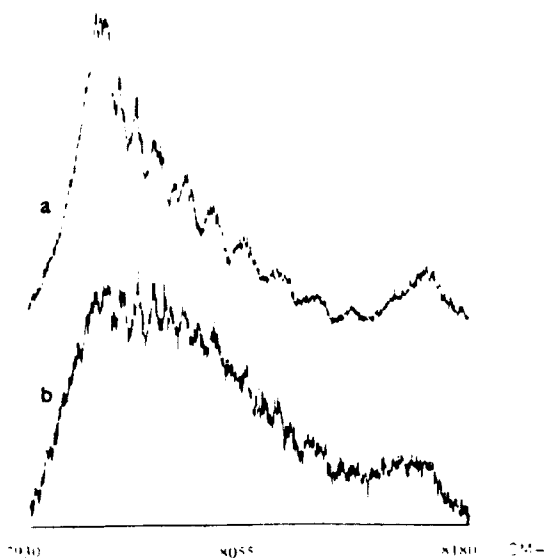


Fig. 4. Details of high-resolution spectra in the IR. (a) Emission: resolution = 0.25 cm^{-1} ; recording time: 2 h 20 min; same conditions of the reaction as in fig. 2. (b) Absorption: resolution = 0.25 cm^{-1} ; recording time: 1 h; same conditions of the cell as in fig. 3.

on the oven temperature and that no LIF was seen until the temperature reached 500°C. Thus, we expect that CuCl_2 is responsible for the fluorescence since these higher temperatures favour its formation over the dimer [15], Cu_2Cl_4 .

Fig. 5 shows the LIF spectra from the two laser lines obtained with the Fourier-transform spectrometer at a resolution of 2 cm^{-1} . These spectra were recorded without filters so that the laser lines themselves are visible in the spectra. We also show a portion of the $\text{O}_2(^1\Delta_g)/\text{Cl}_2/\text{Cu}$ flame spectrum for comparison.

The LIF spectra are composed mainly of multiple series of resolved doublets. The series of doublets marked "O" and "y" have components that coincide with the 676.4 and 647.1 nm laser lines, respectively. The other doublet series in the spectra, "x" for example, do not have components that share the laser excitation frequency. It should be noted that the spacings between most of the stronger doublet series in each spectrum are very similar. We can also see unresolved, regularly spaced clumps in figs. 5a and 5b. There is remarkable similarity to these features

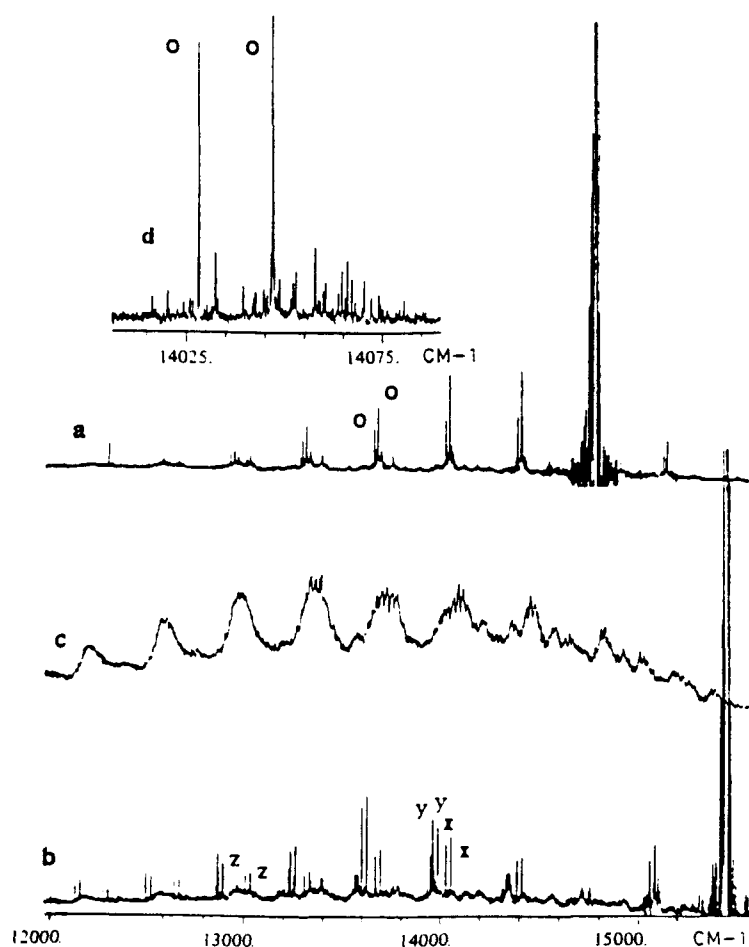


Fig. 5. (a) Fluorescence spectrum from excitation by krypton laser line $\lambda = 676.4\text{ nm}$ (14779.15 cm^{-1}). $P_{\text{laser}} = 0.7\text{ W}$; temperature of the cell: 620°C ; temperature of the sidearm: 370°C ; recording time: 8 h; cell: same conditions as in fig. 3. (b) Fluorescence spectra from excitation by krypton laser line $\lambda = 647.1\text{ nm}$ (15449.56 cm^{-1}). $P_{\text{laser}} = 1.7\text{ W}$; temperature of the cell: 615°C ; temperature of the sidearm: 382°C ; recording time: 3 h; cell: same conditions as in fig. 3. (c) Emission of the Yoshida reaction in the red: same conditions as in fig. 2. (a), (b), (c): plots at 2 cm^{-1} resolution. (d) Detail of spectrum (a): resolution = 0.1 cm^{-1} .

and those found in the $O_2(^1\Delta_g)/Cl_2/Cu$ flame spectrum, seen in fig. 5c. Under the higher resolution displayed in fig. 5d, these clumps are seen to consist of numerous weak lines of which some must certainly correspond to excitation of the less abundant isotopomers of $CuCl_2$ such as $^{35}Cl-Cu-^{37}Cl$. Most of the intense series of doublets have a spacing that corresponds to the symmetric stretch of the $CuCl_2$ ground state: the absence of Q lines allows us to confirm that this state is indeed $^2\Pi_g$ and not $^2\Sigma_g^+$.

The "y" series in the 647.1 nm LIF spectrum extends from 11443 cm^{-1} to an anti-Stokes doublet at 15817 cm^{-1} . The interval between the doublets grows from 356.3 to 367.8 cm^{-1} as frequency increases while the doublet spacing changes from 24.910 to 25.515 cm^{-1} . The doublets split into a set of two doublets with 0.06 cm^{-1} spacing at 14700 cm^{-1} . We expect that this is A-type doubling caused by interaction with the low-lying $^2\Sigma_g^+$ state with the splitting increasing as the ground-state levels approach those of this state, the laser being broad enough (5 GHz) to pump simultaneously both e and f sublevels. If one assumes that the lines at 15817 cm^{-1} correspond to zero quanta in ν_1 , then the last doublets in this series involve a $CuCl_2$ level having twelve quanta of excitation in the symmetric stretch mode.

4. Discussion

Although we are not able to perform an absolute vibrational assignment at present, our LIF data show from our hypothetical numbering, that $\nu'' = 12$ of ν_1 lies at least 4348 cm^{-1} above $\nu'' = 0$. The small variation in the vibrational spacing provides evidence that the well of the ground state of $CuCl_2$ is rather deep and may support many vibrational levels. The LIF spectrum and the red-emission system of the $O_2(^1\Delta_g)/Cl_2/Cu$ flame are taken to be the $^2\Pi_u-^2\Pi_g$ transition of $CuCl_2$. Based upon this assignment, our data provide a lower limit for the $^2\Pi_u$ electronic energy of 15800 cm^{-1} , which is in reasonable agreement with the 16690 cm^{-1} ab initio value [16]. The Kr^+ laser excited one or the other of the spin-orbit sublevels of the $^2\Pi_u$ state, and the LIF is due to emission to the $\Omega = 1/2$ and/or $\Omega = 3/2$ spin-orbit components of the ground state.

In the case of the flame, the $^2\Pi_u$ state must be ex-

cited by a two-step mechanism, requiring two molecules of $O_2(^1\Delta_g)$ to transfer their energy (7880 cm^{-1}) to $CuCl_2$. The first step is to populate the $^2\Delta_g$ state, and the second the $^2\Pi_u$ state. If the total energy transferred is 15760 cm^{-1} , it is clear that only the lowest vibrational levels of the $^2\Pi_u$ state ($T_e \approx 15800\text{ cm}^{-1}$) are likely to be involved in the red flame.

We, therefore, agree with Tokuda et al. [10] that the visible red emission is $^2\Pi_u-^2\Pi_g$ (and possibly $^2\Pi_u-^2\Sigma_g^+$), but we question their explanation of the infrared emission, namely $^2\Pi_u-^2\Delta_g$. We believe that this emission is more likely to arise from $^2\Delta_g-^2\Pi_g$ for the following reasons:

Firstly, there are marked similarities between the emission and absorption spectra taken in the 8000 cm^{-1} region (fig. 4) suggesting that the same electronic states are involved. As the absorption experiment must originate from the lowest-lying electronic states, we are left with the upper state as $^2\Delta_g$ from ref. [16], as mentioned in section 3.

Secondly, we have observed that towards the end of an experimental run, when the $O_2(^1\Delta_g)$ concentration decreases rapidly, the infrared emission around $1.3\text{ }\mu\text{m}$ can be observed when the red emission is extinguished. This would not be the case if both systems involved the same upper state. However, even at low oxygen concentrations, the reservoir state $^2\Delta_g$ of $CuCl_2$ can still emit to lower-lying electronic states. The collisional excitation of $CuCl_2$ $^2\Delta_g$ should be close to first order in $[O_2(^1\Delta_g)]$, whereas the population of the $^2\Pi_u$ state of $CuCl_2$ is at least quadratic in its dependence on $[O_2(^1\Delta_g)]$ [3].

Thirdly, we have not yet managed to record direct LIF in $CuCl_2$ corresponding to $^2\Pi_u-^2\Delta_g$. This should not be regarded as conclusive proof at this stage, though, because the thermal emission from the quartz cell maintained at around 600°C is much stronger than the fluorescence signal.

We had hoped to discover which spin-orbit component of the $^2\Delta_g$ state is involved in the energy transfer from $O_2(^1\Delta_g)$, but this is still an open question. The electronic transition in $CuCl_2$ $^2\Delta_g-^2\Pi_u$ must be close to resonance with $O_2(^1\Delta_g)-O_2(^3\Sigma_g^-)$ (7880 cm^{-1}), and the best calculations of ref. [16] (coupled-pair functional method - CPF) give T_e for $^2\Delta_g$ ($\Omega = 5/2$) as 7514 cm^{-1} . This would provide an excellent relay state, but would imply that the infrared

emission (fig. 2) is due to ${}^2\Delta_g(\Omega=5/2)-{}^2\Pi_g(\Omega=3/2)$ and ${}^2\Delta_g(\Omega=5/2)-{}^2\Pi_g(\Omega=1/2)$. The latter would require some explanation.

Another point of view is that although the CPF calculations of ref. [16] give the best results for the ${}^2\Pi_u$ state, the configuration-interaction calculation with the Davidson correction, labelled SDCI+Q in ref. [16], is better for the ${}^2\Delta_g$ state. Ref. [16] suggests that the true values lie between these two calculations anyway. This being so, the relay would be ${}^2\Delta_g(\Omega=3/2)$ with $T_e=7692\text{ cm}^{-1}$, which is more satisfactory for the spectroscopist, but we would have to explain why, if ${}^2\Delta_g(\Omega=5/2)$ lies at 5498 cm^{-1} , the absorption band of CuCl_2 is found beyond 6000 cm^{-1} . The ambiguity remains.

We were also interested to learn whether or not this system could produce a chemically pumped laser. The vibrational separations observed in the $\text{O}_2({}^1\Delta_g)/\text{Cl}_2/\text{Cu}$ flame spectrum (fig. 5c) are the same as those in the LIF spectra. Thus, a large portion of this red emission is to excited vibrational levels of the CuCl_2 ground state which are not appreciably thermally populated. Hence, there is presumably a population inversion created in the $\text{O}_2({}^1\Delta_g)/\text{Cl}_2/\text{Cu}$ system. We have performed some preliminary time-resolved experiments applying a Cu-vapor pumped dye laser to excited CuCl_2 in the 600–700 nm region. The observed LIF decay, of the order of 90 ns, varied little with excitation wavelength. In addition, the decays were insensitive to pressure and changed little as the sidearm temperature was altered. The measured decay contains contributions from both radiative and non-radiative processes, and we can say little at the present on the oscillator strength of this transition. In any case, these decays are much too short to expect that the $\text{O}_2({}^1\Delta_g)/\text{Cl}_2/\text{Cu}$ system will lead to laser oscillation on this transition. However, the ${}^2\Delta_g-{}^2\Pi_g$ infrared system may have a radiative lifetime of the order of 1.5 μs , since, from absorption spectra, its oscillator strength is about 15 times less than that of the ${}^2\Pi_u-{}^2\Pi_g$ transition. More work is warranted on this system to investigate whether laser action is feasible.

5. Conclusion

A comparison of spectroscopic data obtained from

$\text{O}_2({}^1\Delta_g)/\text{Cl}_2/\text{Cu}$ visible and infrared flame emission and, in separate experiments, from LIF of CuCl_2 strongly indicates that CuCl_2 is responsible for the chemiluminescence. We have assigned this visible emission to the $\text{CuCl}_2\ {}^2\Pi_u-{}^2\Pi_g$ transition. The CuCl_2 infrared absorption spectra are very similar to the flame emission spectra in the 8000 cm^{-1} region, and it is suggested that the ${}^2\Delta_g-{}^2\Pi_g$ transition be assigned to the infrared system. To verify further this hypothesis, we attempted to observe the LIF spectrum in the infrared. However, background blackbody radiation from the oven thwarted our attempts. We are currently modifying our experimental set-up to minimize this parasitic radiation and will record infrared Fourier-transform spectra which will provide the necessary information to characterize the infrared emission. In addition, we are currently using a single-frequency ring dye laser operating in the 700 nm region to record extensive CuCl_2 laser-induced fluorescence Fourier-transform spectra so that a much more complete understanding of the $\text{CuCl}_2\ {}^2\Pi_u-{}^2\Pi_g$ electronic transition will be possible.

Acknowledgement

This work was supported by the DRET Contract No. 901609 and the Fourier-transform spectrometer was largely funded by the CNRS and Université Claude Bernard – Lyon I.

References

- [1] S. Yoshida, M. Taniwaki, T. Sawano, K. Shimizu and T. Fujioka, Japan. J. Appl. Phys. 28 (1989) L831.
- [2] S. Yoshida, K. Shimizu, T. Sawano, T. Tokuda and T. Fujioka, Appl. Phys. Letters 54 (1989) 2400.
- [3] S. Yoshida, T. Tokuda and K. Shimizu, Appl. Phys. Letters 55 (1989) 2707.
- [4] R. Bacis, J. Bonnet, A.J. Bouvier, S. Churassy, P. Crozet, B. Erba, E. Georges, J. Lamarre, Y. Louvet, M. Nota, D. Pigache, A.J. Ross and M. Setra, Europhys. Letters 12 (1990) 569.
- [5] Q. Zhuang, T.J. Cui, F.T. Sang, Q.N. Yuan, R.Y. Zhang, H.P. Yang, Li Li, Q.S. Zhu and C.H. Zhang, Conf. Proc. CLEO/IQEC, Anaheim, California (1990).
- [6] R. Huang, R. Zhang and R.N. Zare, Chem. Phys. Letters 170 (1990) 437.

- [7] N.P. Vagin, A.F. Konoshenko, P.G. Kryukov, M.P. Frolov and N.N. Yuryshv, *Soviet J. Quantum Electron.* 20 (1990) 159.
- [8] Q. Zhuang, T.J. Cui, X.B. Xie, F.T. Sang, Q.N. Yuan, R.Y. Zhang, H.P. Yang, Li Li, Q.S. Zhu and C.H. Zhang, *Conference Proceedings of the 8th International Symposium on Gas Flow and Chemical Lasers, Madrid, Spain (1990)*.
- [9] R. Bacis, J. Bonnet, A.J. Bouvier, S. Churassy, P. Crozet, B. Erba, E. Georges, C. Jouvét, Y. Jouvét, J. Lamarre, M. Nota, D. Pigache, A.J. Ross and M. Setra, *Conference Proceedings of the 8th International Symposium on Gas Flow and Chemical Lasers, Madrid, Spain (1990)*.
- [10] T. Tokuda, N. Fujii, S. Yoshida, K. Shimizu and I. Tanaka, *Chem. Phys. Letters* 174 (1990) 385.
- [11] J.T. Hougen, G.E. Leroi and T.C. James, *J. Chem. Phys.* 34 (1961) 1670.
- [12] G.E. Leroi, T.C. James, J.T. Hougen and W. Klemperer, *J. Chem. Phys.* 36 (1962) 2879.
- [13] C.W. DeKoch and D.M. Gruen, *J. Chem. Phys.* 44 (1966) 4387.
- [14] C.W. DeKoch and D.M. Gruen, *J. Chem. Phys.* 49 (1968) 4521.
- [15] F. Dienstbach, F.P. Emmenegger and C.W. Schlapher, *Helv. Chem. Acta* 60(1977) 2460.
- [16] C.W. Bauschlicher Jr. and B.O. Ross, *J. Chem. Phys.* 91 (1989) 4785.

APPENDIX 5

JOURNAL OF MOLECULAR SPECTROSCOPY (To be published)

THE GROUND STATE OF THE CuCl_2 MOLECULE FROM LASER INDUCED FLUORESCENCE

A.J. Ross, R. Bacis, A.J. Bouvier, S. Churassy, J.-C. Coste, P. Crozet and I. Russier

Laboratoire de Spectrométrie Ionique et Moléculaire,
Bâtiment 205, Université Lyon I,
43, Boulevard du 11 novembre 1918,
69622 Villeurbanne Cedex,
France.

Abstract

The ground state of CuCl_2 has been studied by laser induced fluorescence spectroscopy. CuCl_2 vapour, produced in a sealed quartz cell, was excited with a ring laser operating with DCM or Rhodamine 6G dye. Fluorescence in the region $11000 - 15500 \text{ cm}^{-1}$ was recorded on a Fourier transform spectrometer. Transitions to about 40 vibrational levels of the ground state have been observed. These are identified as vibrational progressions in the symmetric stretch ($0 \leq \nu_1'' \leq 12$) in combination with even quanta of the antisymmetric stretch ($\nu_3'' = 0, 2, 4, 6$ or 8) occurring to the ${}^2\Pi_g$ ground state.

Introduction.

In an earlier paper [1], we presented the results of a laser induced fluorescence experiment, in which the red lines of a krypton ion laser were used to excite CuCl_2 vapour. The spectra were composed of resolved doublets, and gave a vibrational interval varying from 356 to 368 cm^{-1} , in close agreement with the ab initio predictions made by Bauschlicher and Roos [2], but no attempt was made to analyse these spectra any further. The quantity of information to be gleaned from them was very limited, and we have since pursued the problem with a tunable laser source. We aimed to probe systematically a set of vibrational and rotational levels in CuCl_2 with the laser, and to record fluorescence from these levels to the low-lying ligand field states. We rely on the selectivity of the laser line to achieve a rotationally simple spectrum from a hot source : the absorption spectrum of CuCl_2 recorded under these conditions is sufficiently congested as to appear to be a continuum [3]. We hoped that such an experiment would allow us to observe all the vibrational modes of the ground state of CuCl_2 - predicted to be $^2\Pi_g$ [2], and also to locate the higher lying ligand field states, $^2\Sigma_g^+$ and $^2\Delta_g$. Our choice of excitation wavelengths has been such that we have excited rotational energy levels of only two vibrational levels of the upper state, assumed to be the charge transfer state $^2\Pi_u$, and, to date, we have analysed fluorescence to only one low-lying electronic state, which we believe to be $^2\Pi_g(3/2)$. We have observed only two of the normal vibrational modes, namely ν_1'' and ν_3'' , which are respectively the symmetric and antisymmetric stretching vibrations of a symmetric triatomic molecule.

The absence of the degenerate bending vibration in our spectra contrasts with results obtained from electronic spectra of nickel dichloride, which is the closest comparison in terms of electronic structure that we could find in the literature. A low-resolution dispersed fluorescence experiment in NiCl_2 , performed by Zink *et al* [4], showed long progressions in ν_1'' and combinations of $n\nu_1''$ with $2\nu_2''$ following excitation by the 364 nm line from an argon ion laser. Other combinations were also assigned in this work, including

combinations of ν_1'' with $2\nu_3''$, but these bands were relatively weak, and no higher levels involving the antisymmetric stretch, ν_3'' , were assigned. An extensive investigation of the excitation spectra of nickel dichloride around 360 nm [5] and 460 nm [6] obtained with a cold molecular beam also failed to give much information about the antisymmetric stretching vibration. The vibrational structure in the spectrum of NiCl_2 was particularly clear in [6]; the obvious features were a long progression in ν_1' , and a short progression involving the excitation of 2 quanta of the bending vibration, ν_2 . Some spin-orbit structure was apparent in these spectra, and some very weak bands were tentatively assigned as sequence bands in the antisymmetric stretching vibration, with $\nu_3' = \nu_3'' = 1$. In copper dichloride, we observed strong transitions to combination levels of $\nu_1'' + (\text{even})\nu_3''$, but no such combinations with $(\text{even})\nu_2''$, or sequences involving the bending vibration.

In any case, it seems that an investigation of dispersed fluorescence from a 'hot' source is likely to prove useful in the study of transition metal dihalides (for which few high resolution spectra exist), as the information obtained covers high-lying rotational and vibrational energy levels of the ground state, and so complements such data as could be obtained from a cold molecular beam experiment. A full analysis of the rovibrational structure of the transition metal dihalides would provide an important clue as to their electronic and geometric structure in the gas phase, adding to information from elaborate *ab initio* calculations, or measurements of the deflection of molecular beams in an inhomogeneous electric field [7], which have been used to determine whether or not an MX_2 molecule is linear. In this instance, an understanding of the electronic spectra of copper dichloride should also clarify the problem, presented in [1,8], concerning the origin of the red and infrared emission observed when hot copper, chlorine and metastable oxygen react together. This emission was first reported by Yoshida *et al* in 1989 [9], and has been extensively studied since [10-13]. There seems to be agreement that CuCl_2 is at least partly, if not wholly, responsible, but an improvement in the spectroscopic data for copper dichloride would add weight to this hypothesis.

In this paper, we describe the experimental conditions used to record electronic spectra of copper dichloride vapour at high resolution, and then give results of the numerical treatment of the spectral lines which have been assigned to the $^{63}\text{Cu}^{35}\text{Cl}_2$ isotopomer. A simple model which takes into consideration the symmetric and antisymmetric stretching vibrations and their anharmonicities, but allows for no other interaction, is used to derive the vibrational and rotational constants of this molecule.

Experimental details

We prepared CuCl_2 by sealing about 10 mg copper powder (99.9 % pure) with enough chlorine gas to react stoichiometrically to produce CuCl_2 in a quartz cell equipped with Brewster windows and a sidearm. The cell was placed in an oven which allowed the main body of the cell to be maintained at 750°C (at which temperature copper dichloride dimer [14] is reported to be fully dissociated), whilst the sidearm temperature was lower, so that the vapour pressure in the cell could be controlled. Although we were concerned that other stable species such as CuCl and Cu_3Cl_3 might also be formed in the source, and tried to add excess chlorine to compensate this, we found in practice that the quality of the spectra was not greatly affected by differences in the original mixture - good spectra were obtained with either copper or chlorine in slight excess.

Fluorescence spectra were excited with a Spectra Physics ring dye laser (380 D) operating single mode with DCM or Rhodamine 6G dye, and recorded on a Bomem DA3 Fourier transform spectrometer using a silicon avalanche detector. The dye laser wavelength was continuously monitored with a Fizeau wavemeter (Laser Technics 100). The set-up is shown schematically in Figure 1.

The spectra were recorded twice, once at very low resolution, and then at higher resolution. The low resolution survey spectra were important because they enabled us to decide which laser wavelengths actually resulted in a discrete spectrum. Given the expected

complexity of the electronic spectrum of CuCl_2 , and the presence of both possible isotopic species of chlorine and copper in our source, we were not particularly surprised to find that the total fluorescence signal from the cell was totally insensitive to the choice of wavelength, even with a laser linewidth of about 50 MHz. The survey spectra showed us that whilst any laser line could excite a broad continuum emission, only a few select frequencies produced the same continuum with a discrete structure superposed on it. Having found a potentially interesting laser wavelength, we went on to record the fluorescence spectrum from 11000 - 15400 cm^{-1} at an apodised resolution of 0.07 cm^{-1} , using an appropriate optical filter to attenuate or eliminate the laser line. The recording time was typically 2 hours.

Experimental results.

The first obvious result was the sensitivity of the discrete part of the spectrum to the choice of the exciting laser wavelength, as illustrated in Figure 2. Our first high resolution recordings of the discrete part of the spectrum, which were obtained using DCM dye, showed a very simple rotational structure (P,R doublets with no relaxation), and an apparently straightforward vibrational pattern (see Figure 3a). It was difficult to ascertain which isotopomer we were seeing, and also to establish rotational numbering from so few lines. In order to facilitate the subsequent analysis, we deliberately chose to use small intervals between our excitation lines, hoping to excite neighbouring rotational levels of a single upper state vibrational level in successive recordings. We concentrated on regions with the laser close to 657 and 647 nm (DCM, with average output power ~ 350 mW), and then worked at higher excitation energies around 607 nm (Rhodamine 6G, power ~200 mW). The discrete fluorescence was spread over about forty vibrational levels of the ground state. The obvious vibrational structure seen in the fluorescence spectra excited by DCM was a progression in the symmetric stretch vibration (Figure 3a), but a more complex vibrational pattern was apparent in the R6G spectra (Figure 3b).

We found that most of our data could be understood in terms of fluorescence from a $T'_{v,J}$ level to the ground state as progressions in the symmetric stretching vibration, occurring in combinations with even quanta of v_3'' (the antisymmetric stretch vibration). The lower energy laser lines (DCM) excited a vibrational level about 15880 cm^{-1} above the lowest level observed in fluorescence, and produced emission essentially to $v_3'' = 0$ and 2, as illustrated in Figure 3a. The Rhodamine 6G excitations were to a different upper state vibronic level, about 370 cm^{-1} higher than the other, and resulted in emission to higher combinations of v_3'' : we have observed bands with $v_3'' = 0, 2, 4, 6$ and 8, (Figure 3b). We assign this emission to part of the ${}^2\Pi_u - {}^2\Pi_g$ transition in CuCl_2 : the only electronic state likely to be excited by the laser, according to the *ab initio* calculations of [2], is ${}^2\Pi_u$, and the P,R doublets observed in fluorescence are consistent with a ${}^2\Pi - {}^2\Pi$ transition. The question remains as to which spin-orbit component is observed. The apparent lack of lambda doubling in the regular parts of the spectrum, even at high J values, tends to suggest that we have observed the ${}^2\Pi_{u(3/2)} - {}^2\Pi_{g(3/2)}$ transition rather than the ${}^2\Pi_{u(1/2)} - {}^2\Pi_{g(1/2)}$ transition (lambda doubling is usually larger in the 1/2 than in the 3/2 component of a ${}^2\Pi$ state). However, this can only be hypothesis until the other component of the ${}^2\Pi_g$ state is observed and characterized, and for the time being we have considered rotational lines to have an effective rotational quantum number J, and have neglected the effects of the orbital angular momentum quantum number Ω . Through lack of information on v_2 , we have also been obliged to neglect the contribution to angular momentum l_2 , which comes from the degenerate bending vibration. Given the absence of progressions in even quanta of the bending vibration in our spectra, we consider it likely that both the upper and lower electronic states of CuCl_2 are linear in geometry.

From our measurements of the antisymmetric stretch $\tilde{\nu}_3''$, we were able to recognize the different isotopomers of CuCl_2 present in our source. This was important, because in some of the DCM spectra, in which only the symmetric stretch progressions were visible, we were unable to distinguish between the two isotopes of copper. So far, we have

observed $^{63}\text{Cu}^{35}\text{Cl}_2$, $^{65}\text{Cu}^{35}\text{Cl}_2$, $^{63}\text{Cu}^{35}\text{Cl}^{37}\text{Cl}$ and $^{65}\text{Cu}^{35}\text{Cl}^{37}\text{Cl}$, but at present most of our data relates to the most common species, $^{63}\text{Cu}^{35}\text{Cl}_2$. The analysis presented here therefore treats only this isotopomer, but work is in progress to acquire a comparable data set for the other species of CuCl_2 .

Data reduction.

In some respects, we suffered from the oversimplification of the rotational structure in our spectra. It was very easy to recognize the spectral features which appeared, but it was much more difficult, if not impossible, to assign all the quantum numbers with certainty, particularly because the regularity of the spectra seen at a first glance (Figures 3a, 3b) is in reality less than perfect - small perturbations abound in the higher v levels. By accumulating some 50 spectra, we eventually assembled the pieces of the puzzle which could be made to fit together, and produced a model which could account for most of the lines observed. However, it must be said that our analysis is not exhaustive. Not having observed the first lines of the rotational bands, we cannot categorically state which spin-orbit component we have studied, neither can we justify fully the vibrational numbering scheme given. One obvious remedy would be to use isotope effects to confirm the numbering presented here, and we intend to work with enriched $^{37}\text{Cl}_2$ to study $\text{Cu}^{37}\text{Cl}_2$ in the near future. For the moment, we have assigned a few lines to $^{65}\text{Cu}^{35}\text{Cl}_2$, which tends to confirm the numbering for the antisymmetric stretch, but is unfortunately of no help for the numbering of the symmetric stretch levels. But we have accrued a data set of some 2000 lines assigned to $^{63}\text{Cu}^{35}\text{Cl}_2$, and can derive from this a fair description of the lower electronic state observed. The rotational analysis was based on the first six levels of the symmetric stretching vibration, which had regular rotational and vibrational spacings. The rotational quantum number defined in this way allows us to represent the rotational energy levels by a simple $B_{\text{eff}} J(J+1) - D_{\text{eff}} J^2(J+1)^2$ expression, and ignores the correction for the (unknown) Ω and the bending vibration's contribution to the total angular momentum.

The extent and number of perturbed lines in the higher vibrational levels observed led us to exploit the data available in two different ways. The first was a fit on a band-by-band basis to a set of effective spectroscopic constants, and the second was to fit the data to a very small set of parameters, which expressed the rovibrational energy levels by a polynomial expression describing the rotation, symmetric and antisymmetric stretching vibrational energies simultaneously. In both cases, the upper state was reduced to a simple expression in T' , B' and D' for the two observed vibrational levels, but no true analysis of the upper state has been attempted. The spread of rotational lines over the observed vibrational levels is indicated in Table 1, but it is important to remember that a laser induced fluorescence experiment does not afford a statistical distribution over rotational levels. In fact, we did not observe any lines at all with $76.5 < J < 108.5$, but levels with $J < 76.5$ were well represented.

The lines included in our data set came from two vibrational levels of what we have assumed to be the $^2\Pi_u$ state. The lower of the two, called level 1, gave a systematic Franck-Condon intensity minimum at $v_1'' = 3$ in our symmetric stretch fluorescence progression, and the higher (level 2) gave two such minima at $v_1'' = 3$ and 7. A small number of lines at high J were also observed as progressions in the symmetric stretch from another level, located about 330 cm^{-1} below level 1, always with $v_3'' = 0$. As we were unable to tell which copper isotope was observed, or confirm that exactly the same lower state levels were involved in these DCM induced transitions, none of these lines were included in our data set. Using fluorescence to four regular lower state levels, we determined effective constants for these two upper state levels with respect to $G_{(v_1''=0, v_3''=0)}$, the lowest observed vibrational level of the ground state. We found :

$$\text{level 1 : } T' = 15882.155 (5) \quad B' = 0.051764 (9) \quad \text{and } D' = 8.41 (77) \times 10^{-9} \text{ cm}^{-1}$$

$$\text{level 2 : } T' = 16257.092 (3) \quad B' = 0.051330 (9) \quad \text{and } D' = 8.45 (79) \times 10^{-9} \text{ cm}^{-1}$$

From the intensity distribution in the progression in v_1'' with $v_3'' = 0$, we were tempted to consider these levels as $v_1' = 1$ and 2 in the upper state. However, the predicted vibrational spacing in the upper state is only 275 cm^{-1} [2], and the observed spacing, $\sim 375 \text{ cm}^{-1}$, is closer to the upper state antisymmetric stretch frequency. So far, attempts to reproduce observed intensities with simple Franck Condon overlap calculations have failed.

Band by band fit.

This approach allowed lower state effective spectroscopic constants to be determined, and gives a fit to the observed lines to better than 0.01 cm^{-1} in the unperturbed levels. We proceeded by fixing the constants for the upper state levels to the values cited above, and in so doing fixed the energy origin to be the lowest observed vibrational level of the ground state. The numerical results are given in Table 2. It becomes obvious that the evolution of the vibrational energies becomes irregular at $v_1'' > 7$ with $v_3'' = 0$, but levels of comparable energy with $v_3'' = 2$ are still reasonably regular. The set of levels with $v_3'' = 2$ becomes noticeably perturbed beyond $v_1'' = 6$, and the observed levels with $v_3'' = 4, 6$ and 8 appear reasonably regular throughout. It is also clear from this table that the values of the effective rotational constants are not greatly affected by these perturbations; their values vary in the usual way.

Some explanation is required concerning the levels for which the standard deviation of the fit is particularly large. These were characterized by the large number of extra lines observed in a few $v' \rightarrow v_1'', v_3''$ bands, illustrated for instance in Figure 4. Trying to fit the lines in these bands to our simple model resulted in a distribution of residuals which was not random, but increased slowly with J . The calculated wavenumber was usually quite close to the average wavenumber of the lines of a given lower state rotational quantum number, as though we were seeing an exaggerated form of lambda-type doubling. This splitting of

interaction which allows us to see multiple lines in certain bands (Figure 4), causes major problems in an overall representation of the energy levels observed. We thus restricted the data set for this polynomial approach to a smaller number of bands, with a view to obtaining parameters which have physical significance for the normally behaved levels. The results obtained are given in Table 3. Two series of constants are given. The first is the fit of a rather restricted set of data, concerning essentially the lower state levels with $v_1'' < 8$, but from which fluorescence to the levels ($v_1'' = 4, v_3'' = 6$), ($v_1'' = 4, v_3'' = 4$) and ($v_1'' = 7, v_3'' = 2$) had also been eliminated. This data set contains essentially unperturbed lines, and the R.M.S. error reflects this (0.14 cm^{-1} for 1517 input lines). The bands which were removed from the total data set were those which had either a RMS error in the band-by-band fit greater than 0.15 cm^{-1} , which was symptomatic of levels in which the rotational lines appeared as doublets (or higher multiplets), particularly at high J, or those for which the vibrational term energy seemed irregular. For example, the lower state level with ($v_1'' = 7, v_3'' = 2$) has a modest r.m.s. error in the band-by-band fit, but when included in the data set for a fit to a polynomial expression, almost all the fluorescence lines to this level were recalculated about 0.4 cm^{-1} from their measured wavenumbers. This reflects a shift of the vibrational energy as a whole. The larger data set appearing in table 3 contains levels with $v_1'' = 10, 11$ and 12 in addition to the data contained in the small data set. Higher anharmonicity terms can just be determined. The differences in the upper state vibronic energies quoted in tables 2 and 3 arise from the implicitly different energy origins for the two fits. The band-by-band fit used the lowest observed vibrational energy level of the ground state as zero energy, whereas the polynomial model has an energy origin corresponding to $v_1'' = v_3'' = -1/2$. This quantity does not reflect a real zero-point energy for the molecule, because the contribution in v_2 has been neglected.

rotational levels, which is important in only 6 of the 40 lower state vibrational levels we have observed, namely (v_1'', v_3'') being (8,0), (9,0), (8,2), (9,2), (4,4) and (4,6), probably arises from strong interactions between the vibrational levels of the other ligand field states. The 'other' spin orbit component of the ${}^2\Pi_g$ state is expected to have very similar spectroscopic constants to the one we see, and to lie close in energy to it, and should thus influence even the lowest vibrational levels. According to the *ab initio* calculations in [2], the observed perturbed levels lie well below the ${}^2\Delta_g$ state, (situated approximately 5000 cm^{-1} above the ground electronic state), so the ${}^2\Sigma_g^+$ state remains the most likely candidate to undergo strong interactions with the ${}^2\Pi_g$ state in this way. Even so, interactions between a ${}^2\Pi_g$ and a ${}^2\Sigma_g^+$ state cannot account for all the observed extra lines, as up to eight lines are observed instead of the usual rotational doublet.

Polynomial fit.

In order to derive the vibrational constants for CuCl_2 , we used a more compact set of parameters to represent the spectroscopic term values, by fitting the measured wavenumbers to an expression of the form $\tilde{\nu}_{\text{measured}} = T(v, J) - T''(v_1'', v_3'', J'')$, in which the energy levels for the lower state were represented by :

$$\begin{aligned} T''(v_1'', v_3'', J'') &= \omega_1 (v_1 + 1/2) + x_{11} (v_1 + 1/2)^2 + x_{111} (v_1 + 1/2)^3 \\ &+ \omega_3 (v_3 + 1/2) + x_{33} (v_3 + 1/2)^2 + x_{333} (v_3 + 1/2)^3 \\ &+ x_{13} (v_1 + 1/2) (v_3 + 1/2) \\ &+ \{B_e - \alpha_1 (v_1 + 1/2) - \alpha_3 (v_3 + 1/2)\} J (J+1) \\ &- DJ^2 (J+1)^2. \end{aligned}$$

However, the results from the band-by-band fit had made it obvious that an attempt to represent the full data set by such a simple expression would be doomed to failure, as the distribution of errors in the recalculated wavenumbers is not at all random. Obviously, the

Discussion.

In this work, we have endeavoured to understand the electronic transitions occurring in laser induced fluorescence spectra of copper dichloride. The nature of the spectra made this task non-trivial, and even now, our picture of the ground state remains incomplete. Some of the omissions require a few words of explanation. One of the more obvious flaws in this study is that we have found no evidence at all for the bending vibration, ν_2 . An absence of progressions in ν_2 can be explained away by claiming that both electronic states involved in the transition are linear, and that wavefunction overlaps with $\Delta\nu_2 \neq 0$ are very small, but even so, we would have expected to see transitions with $\Delta\nu_2 = 0$ corresponding to $\nu_2 = 1, 2$ etc. The bending vibration has been measured at 127 cm^{-1} [14] in the ground state, and using DCM dye, we have recorded many fluorescence series originating from a ground state level with $\nu_1 = 1$, which is roughly equivalent in energy to three quanta of ν_2 . There is thus no reason to suppose that the levels $\nu_2 = 1, 2$ and 3 are not thermally populated at the temperatures of our experiment ($\sim 750 \text{ }^\circ\text{C}$). The most probable, although not very satisfactory, explanation for this may well lie in our choice of laser wavelengths. Because we had aimed to produce a data set which was 'easy' to analyse, we worked over a fairly small range of laser wavelengths within the profile of each dye. It is just possible that the difference between the upper and lower state stretching frequencies is large enough for transitions with - say - $\nu'_2 = \nu''_2 \neq 0$ to have been inaccessible to our excitation lines. The same reasoning can be applied to our failure to observe the other spin-orbit component of the ${}^2\Pi_g$ state with a little more confidence : it is not unreasonable to postulate that the energy origins of the ${}^2\Pi_{u(3/2)} - {}^2\Pi_{g(3/2)}$ and ${}^2\Pi_{u(1/2)} - {}^2\Pi_{g(1/2)}$ transitions could be separated by more than 50 cm^{-1} by spin-orbit effects in the CuCl_2 molecule.

With these limitations in mind, we have analysed the vibrational features in our fluorescence spectra, and obtained reliable spectroscopic constants for rotational motion, and for the symmetric and antisymmetric stretching vibrations. We have observed two vibronic

levels of the upper state, whose identities in terms of vibrational modes remain obscure, and we have assigned the discrete lines in the fluorescence spectrum to transitions from these levels to a single lower lying electronic state of CuCl_2 . But the discrete part of the spectrum is in fact a minor component of the total fluorescence (see figure 2). The origin of the ever-present continuum is not at all clear. It might arise from collisional transfer of energy to neighbouring electronic states, but if energy transfer were to occur whilst CuCl_2 is in its $^2\Pi_u$ excited state, we would normally have seen extensive rotational relaxation lines around the main fluorescence doublets, as well as the collisionally excited continuum transition. Another hypothesis is that the continuum emission comes from CuCl_2 dimers, which might either be excited directly by the laser ($(\text{CuCl}_2)_2$ has been reported [14] to absorb quite strongly around 600 nm), or else be formed by collision between a CuCl_2 molecule in the $^2\Pi_u$ state and a ground state molecule. Whatever its origin, this continuum can be produced by any wavelength issuing from the ring laser operating with R6G or DCM. Although this discovery seems simply to add yet another unanswered question, it was an interesting observation for another reason.

The original choice of copper dichloride as a transition metal dihalide for spectroscopic investigation was influenced by our attempts to identify the emitting species in the reaction between hot copper and chlorine in the presence of singlet oxygen ($^1\Delta_g$). The bright red emission which accompanies this reaction was first reported by Yoshida et al [9], and has since been studied by many other groups [10-13]. We had recorded this emission on our FT spectrometer from 650 - 900 nm. The emission consists of a continuum with broad vibrational peaks superposed on it. We supported the hypothesis that copper dichloride was responsible for this emission, but could not eliminate the possibility that more than one species might be involved. Now we find that the fluorescence lines from our upper level "1" to the observed component of the $^2\Pi_g$ state of CuCl_2 match the peaks in the emission spectrum of the red flame, and that the continuum found in the fluorescence spectra matches the continuum of the flame rather well. We intend to pursue this aspect further once we have more data pertaining to the other isotopomers of copper dichloride.

Conclusion

We have used a simple laser induced fluorescence technique in combination with a traditional hot source to produce very simple, rotationally resolved electronic spectra of copper dichloride. Fourier transform spectra extending from 11000 to 15500 cm^{-1} revealed vibrational progressions in the totally symmetric vibration, ν_1'' , and also in even quanta of the antisymmetric vibration, ν_3'' . The non-appearance of vibrational levels with $\nu_3'' = 1, 3, 5$ etc is governed by the symmetry of this linear molecule. Given that ν_2 and ν_3 are non-totally symmetric vibrations, only transitions with even $\Delta\nu_3$ and $\Delta\nu_2$ can exist in a progression, because the total vibrational wavefunction must be totally symmetric for the transition to be allowed. Usually, the intensity of the progression in even $\Delta\nu_3$ drops rapidly as ν_3 increases. We cannot yet explain why we observe such a strong divergence from normal behaviour in this respect. Progressions in even quanta of ν_2 , which are symmetry allowed, are likely to be weak if both the upper and lower electronic states are linear, as overlap between the upper and lower state wavefunctions will be poor. We observed neither progressions nor combinations in the bending vibration.

Having identified the vibrational structure present in our fluorescence spectra, we derived molecular constants for the ground state, $^2\Pi_g$ of the $^{63}\text{Cu}^{35}\text{Cl}_2$ molecule, both on a band-by-band basis, and in the form of a simple polynomial expression. The differences between the energies associated with the three normal vibrational modes are such that we have been able to ignore Fermi resonances at this stage, and can represent the vibrational energies of levels up to about 2500 cm^{-1} ($\nu_1'' < 8$) involving the symmetric and antisymmetric stretching vibrations by their fundamental frequencies and first order anharmonicity terms. Only the anharmonicity constant x_{13} couples these two vibrations in this model, which nonetheless recalculates all fluorescence lines occurring to these vibrational levels to within 0.15 cm^{-1} .

Acknowledgements

We should like to thank Mr B. Erba who made a series of CuCl_2 cells for us. We are also grateful to Dr J.M. Brown and his collaborators for helpful discussions based on their experience with nickel dichloride, and to Dr C. Linton for his critical reading of the manuscript. The Fourier transform interferometer was financed jointly by the CNRS, Université Lyon I and the Région Rhone Alpes. This work benefited from financial support from the Air Force Office of Scientific Research (grant AFOSR-91-0235) and from the Direction des Recherches, Etudes et Techniques, (grant 901609 / A000 / DRET / DS / SR).

Table 1. Range of J" values observed.

$v_1'' \backslash v_3''$	0	2	4	6	8
0	16 ¹ / ₂ - 75 ¹ / ₂	8 ¹ / ₂ - 110 ¹ / ₂	8 ¹ / ₂ - 110 ¹ / ₂	35 ¹ / ₂ - 75 ¹ / ₂	
1	25 ¹ / ₂ - 75 ¹ / ₂	8 ¹ / ₂ - 110 ¹ / ₂	6 ¹ / ₂ - 110 ¹ / ₂	8 ¹ / ₂ - 75 ¹ / ₂	41 ¹ / ₂ - 73 ¹ / ₂
2	18 ¹ / ₂ - 57 ¹ / ₂	16 ¹ / ₂ - 110 ¹ / ₂	7 ¹ / ₂ - 110 ¹ / ₂	8 ¹ / ₂ - 75 ¹ / ₂	41 ¹ / ₂ - 75 ¹ / ₂
3	7 ¹ / ₂ - 110 ¹ / ₂	16 ¹ / ₂ - 110 ¹ / ₂	8 ¹ / ₂ - 110 ¹ / ₂	6 ¹ / ₂ - 75 ¹ / ₂	47 ¹ / ₂ - 73 ¹ / ₂
4	7 ¹ / ₂ - 110 ¹ / ₂	7 ¹ / ₂ - 110 ¹ / ₂	9 ¹ / ₂ - 110 ¹ / ₂	8 ¹ / ₂ - 75 ¹ / ₂	45 ¹ / ₂ - 64 ¹ / ₂
5	18 ¹ / ₂ - 110 ¹ / ₂	7 ¹ / ₂ - 75 ¹ / ₂	35 ¹ / ₂ - 110 ¹ / ₂	8 ¹ / ₂ - 75 ¹ / ₂	45 ¹ / ₂ - 62 ¹ / ₂
6	8 ¹ / ₂ - 75 ¹ / ₂	7 ¹ / ₂ - 75 ¹ / ₂		43 ¹ / ₂ - 75 ¹ / ₂	
7	7 ¹ / ₂ - 75 ¹ / ₂	7 ¹ / ₂ - 75 ¹ / ₂			
8	7 ¹ / ₂ - 75 ¹ / ₂	8 ¹ / ₂ - 75 ¹ / ₂			
9	7 ¹ / ₂ - 110 ¹ / ₂	7 ¹ / ₂ - 75 ¹ / ₂			
10	7 ¹ / ₂ - 110 ¹ / ₂	8 ¹ / ₂ - 75 ¹ / ₂			
11	9 ¹ / ₂ - 110 ¹ / ₂	8 ¹ / ₂ - 75 ¹ / ₂			
12	8 ¹ / ₂ - 75 ¹ / ₂	45 ¹ / ₂ - 64 ¹ / ₂			

List of references.

- 1 A.J. Bouvier, R. Bacis, J. Bonnet, S. Churassy, P. Crozet, B. Erba, J.B. Koffend, J. Lamarre, M. Lamrini, D. Pigache and A.J. Ross Chem. Phys. Lett. 133 184 (1991)
- 2 C.W. Bauschlicher and B.O. Roos J. Chem Phys 91 4785 (1989)
- 3 C.W. Decock and D.M. Gruen J. Chem. Phys. 44 4387 (1966)
- 4 L.R. Zink, J.M. Brown, T.R. Gilson and I.R. Beattie Chem. Phys. Lett. 146 501 (1988)
- 5 L.R. Zink F.J. Grieman, J.M. Brown J. Mol Spectr. 146 225 (1991)
- 6 S.Ashworth, F.J. Grieman and J.M. Brown Chem. Phys. Lett. 175 660 (1990)
- 7 A. Büchler, J. Stauffer and W. Klemperer J. Chem. Phys. 40 3471 (1964)
- 8 A.J. Bouvier , R. Bacis, J. Bonnet, S. Churassy, P. Crozet, B. Erba, J.B. Koffend, J. Lamarre, M. Lamrini, D. Pigache and A.J. Ross J. de Physique IV C7-663 (1991)
- 9 S. Yoshida , M. Taniwaki, T. Sawano, K. Shimizu and T. Fujioka J. Appl. Phys. Japan. 28 L831 (1989)
- 10 S. Yoshida, K. Shimizu, T. Sawano, T. Tokuda and T. Fujioka Appl. Phys. Lett 54 2400 (1989)
- 11 T. Tokuda, N. Fujii, S. Yoshida, K. Shimizu and I. Tanaka Chem. Phys. Lett 174 385 (1990)
- 12 R. Bacis, J. Bonnet, A.J. Bouvier, P. Crozet, S. Churassy, E. Georges, B. Erba, J. Lamarre, ~~J. Lamarre~~, Y. Louvet, M. Nota, D. Pigache, A.J. Ross and M. Setra Europhysics Lett. 12 569 (1990)
- 13 H.P. Yang, Y. Qin, T.J. Cui, Q.N. Yuan, X.B. Xie, Q. Zhuang and C.H. Zhang Chem. Phys. Lett. 191 130 (1992)
- 14 F. Dienstback, F.P. Emmenegger and C.W. Sclapher Helv. Chem. Acta 60 2460 (1977)

Table 2. Constants from band by band fit of fluorescence lines of $^{63}\text{Cu}^{35}\text{Cl}_2$.

v_1''	v_3''	G_{v_1, v_3} cm^{-1}	B_{v_1, v_3} cm^{-1}	$10^9 D_{v_1, v_3}$ cm^{-1}	N° lines	Rms. dev. cm^{-1}
0	0	0.0	0.058161 (3)	10.0	4	0.009
1	0	369.392 (3)	0.058024 (3)	7.8 (4)	9	0.003
2	0	737.755 (3)	0.057914 (7)	10.5 (17)	18	0.005
3	0	1105.140 (3)	0.057691 (1)	6.2 (1)	50	0.010
4	0	1471.471 (3)	0.057648 (1)	6.5 (1)	84	0.011
5	0	1836.788 (2)	0.057516 (1)	5.5 (1)	39	0.006
6	0	2201.083 (6)	0.057379 (6)	6.1 (10)	105	0.023
7	0	2564.354 (23)	0.057215 (7)	10.0	127	0.132
8	0	2926.450 (160)	0.057270 (56)	10.0	116	0.961
9	0	3288.026 (86)	0.057218 (22)	10.0	120	0.554
10	0	3647.980 (12)	0.057055 (6)	9.5 (6)	89	0.051
11	0	4007.137 (7)	0.056897 (3)	7.3 (3)	47	0.018
12	0	4365.262 (5)	0.056753 (4)	4.3 (7)	37	0.012
0	2	1042.005 (4)	0.057739 (2)	6.0 (2)	45	0.013
1	2	1406.267 (3)	0.057620 (1)	6.1 (1)	62	0.011
2	2	1769.493 (4)	0.057502 (3)	6.5 (2)	29	0.011
3	2	2131.680 (3)	0.057379 (2)	7.5 (1)	61	0.011
4	2	2492.690 (39)	0.057427 (20)	18.1 (18)	60	0.158
5	2	2853.004 (3)	0.057133 (2)	3.7 (4)	82	0.010
6	2	3212.052 (6)	0.057004 (4)	6.3 (8)	102	0.021
7	2	3570.065 (31)	0.056860 (27)	7.4 (46)	72	0.106
8	2	3926.810 (300)	0.056771 (86)	10.0	89	1.33
9	2	4283.164 (342)	0.056726 (105)	10.0	78	1.44
10	2	4637.790 (34)	0.056697 (27)	6.5 (46)	57	0.097
11	2	4991.582 (16)	0.056543 (12)	7.6 (20)	36	0.036
12	2	5344.303 (3)	0.056417 (1)	10.0	3	0.001

Table 2 / continued

ν_1''	ν_3''	G_{ν_1, ν_3} cm ⁻¹	B_{ν_1, ν_3} cm ⁻¹	$10^9 D_{\nu_1, \nu_3}$ cm ⁻¹	N° lines	Rms. dev. cm ⁻¹
0	4	2074.366 (2)	0.057343 (1)	5.9 (1)	48	0.008
1	4	2433.585 (2)	0.057224 (1)	6.1 (1)	59	0.007
2	4	2791.753 (2)	0.057101 (1)	6.2 (1)	67	0.009
3	4	3148.835 (2)	0.056974 (9)	7.7 (1)	61	0.007
4	4	3504.892 (19)	0.057066 (62)	22.2 (49)	46	0.348
5	4	3859.885 (22)	0.056773 (9)	6.1 (6)	13	0.020
0	6	3097.104 (10)	0.056973 (6)	9.2 (9)	18	0.007
1	6	3451.393 (4)	0.056827 (3)	5.8 (5)	40	0.007
2	6	3804.548 (3)	0.056703 (2)	6.1 (4)	61	0.008
3	6	4156.506 (6)	0.056612 (6)	13.8 (10)	63	0.021
4	6	4507.220 (110)	0.056695 (36)	10.0	74	0.506
5	6	4857.481 (27)	0.056429 (7)	10.0	48	0.081
6	6	5206.296 (18)	0.056243 (10)	5.2 (13)	23	0.008
1	8	4459.689 (16)	0.056456 (1)	8.9 (1)	13	0.006
2	8	4807.880 (20)	0.056323 (11)	8.0 (1)	22	0.009
3	8	5154.764 (52)	0.056166 (12)	10.0	13	0.032
4	8	5501.228 (1)	0.056123 (1)	10.0	4	0.005

The figures given in parenthesis represent one standard deviation, in units of the last quoted digit. It was not always possible to determine the distortion constant, D_{ν_1, ν_3} . When necessary, we fixed D_{ν_1, ν_3} at 10^{-8} cm⁻¹, in which case no error is given.

Table 3.

Molecular constants (in cm^{-1}) of $^{63}\text{Cu}^{35}\text{Cl}_2$ obtained from fit to polynomial expression.

	Small data set ($v_1'' < 8$)	Larger data set ($v_1'' < 12$)
ω_1	371.669 (11)	371.885 (22)
x_{11}	- 0.5143 (10)	- 0.5604 (38)
x_{111}	-	$2.7 (2) \times 10^{-3}$
ω_3	525.681 (9)	525.878 (25)
x_{33}	- 1.1762 (8)	- 1.107 (6)
x_{333}	-	$-5.7(5) \times 10^{-3}$
x_{13}	- 2.542 (1)	- 2.555 (2)
B_e	0.05831 (1)	0.05827 (1)
α_1	$1.25 (1) \times 10^{-4}$	$1.14 (1) \times 10^{-4}$
α_3	$1.95 (1) \times 10^{-4}$	$1.86 (2) \times 10^{-4}$
D_e	$9.1 (15) \times 10^{-9}$	$13.3 (21) \times 10^{-9}$
N° lines	1517	1829
RMS deviation	0.14	0.25
T' (level 1)	16329.59 (3)	16329.70 (6)
T' (level 2)	16704.54 (3)	16704.62 (6)

The rotational constants B_v' and D_v' for the upper state levels 1 and 2 were kept fixed at the values determined from the band by band fit (see text).

Level 1 : $B' = 0.051764$, $D' = 8.41 \times 10^{-9}$ Level 2 : $B' = 0.051330$, $D' = 8.45 \times 10^{-9}$

Captions to Figures.

Figure 1 : Experimental set-up. BS1 and BS2 are beamsplitters, used to direct part of the laser beam to a mode analyser (MA) and to a Fizeau wavemeter. M is a pierced mirror which collects backwards fluorescence from the CuCl_2 cell. L is a quartz lens, $f=20$ cm. OF represents 10m fused silica optical fibre, which transfers the fluorescence to the Fourier transform spectrometer. The cell is maintained at 750 °C, with the sidearm at 550 °C.

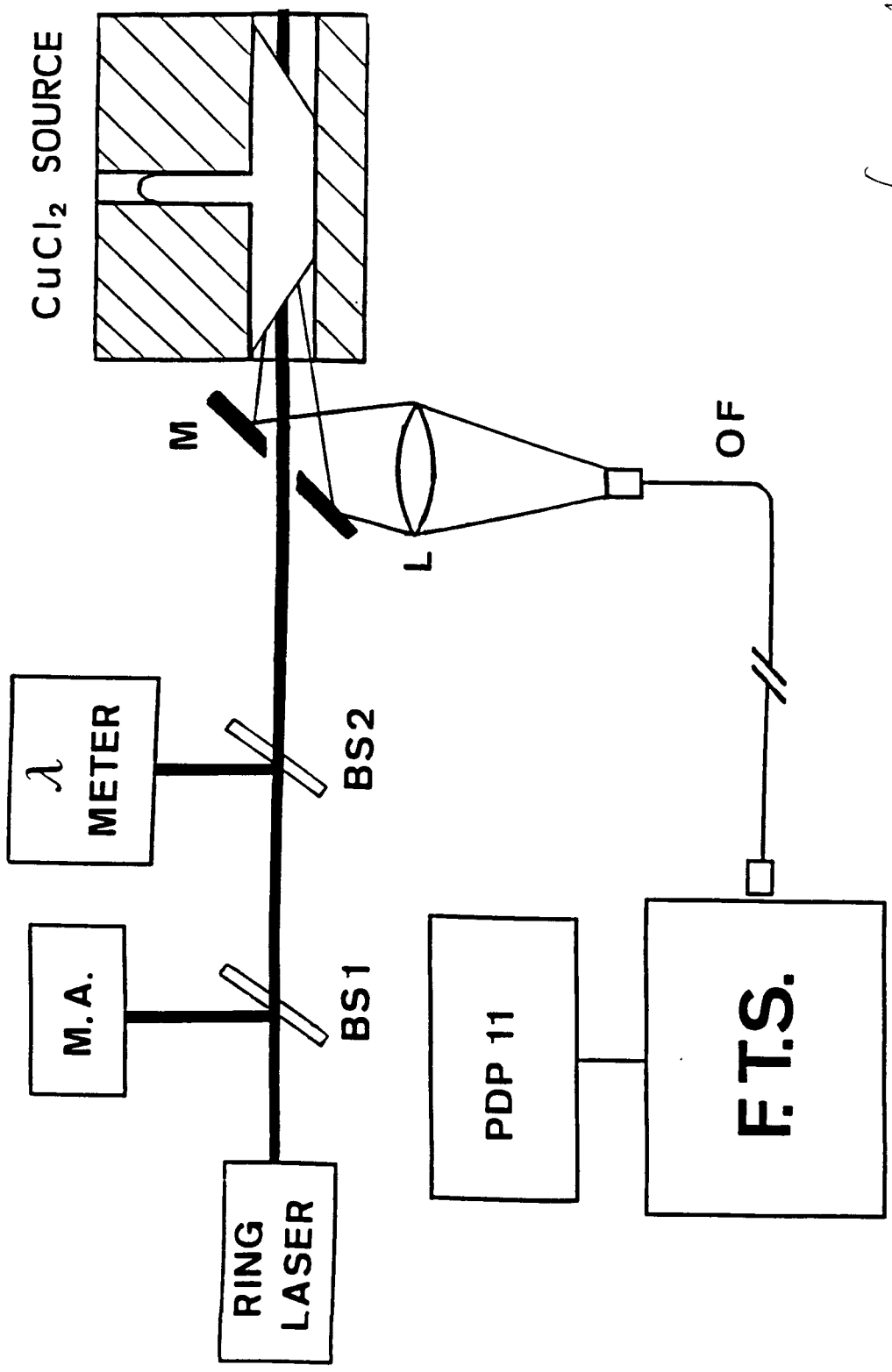
Figure 2 : A series of low resolution ($\sim 30 \text{ cm}^{-1}$) spectra, showing the sudden appearance of a discrete spectrum as the excitation wavenumber changes. From top to bottom, the laser was set at 16229.26 cm^{-1} , 16229.23 cm^{-1} , 16229.20 cm^{-1} , and 16229.16 cm^{-1} .

Figure 3 : Examples of resolved fluorescence spectra, giving vibrational numbering in ν_1'' at given ν_3'' .

3a: Spectrum recorded at 0.08 cm^{-1} resolution with the ring laser operating at 15502.3 cm^{-1} with DCM dye, exciting $J' = 31\frac{1}{2}$ in 'Level 1' (see text).

3b: Spectrum recorded at 0.07 cm^{-1} resolution with the ring laser operating at 16236.60 cm^{-1} with R6G dye, exciting $J' = 46\frac{1}{2}$ and $63\frac{1}{2}$ in 'Level 2'(see text).

Figure 4 : Detail taken from figure 3b, showing obvious perturbations in the band with $\nu_1'' = 8$, $\nu_3'' = 0$, whilst the nearby $\nu_1'' = 5$, $\nu_3'' = 2$, and $\nu_1'' = 2$, $\nu_3'' = 4$, remain regular. The laser pumps both $J' = 46\frac{1}{2}$ and $63\frac{1}{2}$ in the upper state vibrational level. Fluorescence doublets from $J' = 46\frac{1}{2}$ are indicated by filled circles, and from $J' = 63\frac{1}{2}$ by open circles.



CuCl₂ SOURCE

Fig. 1

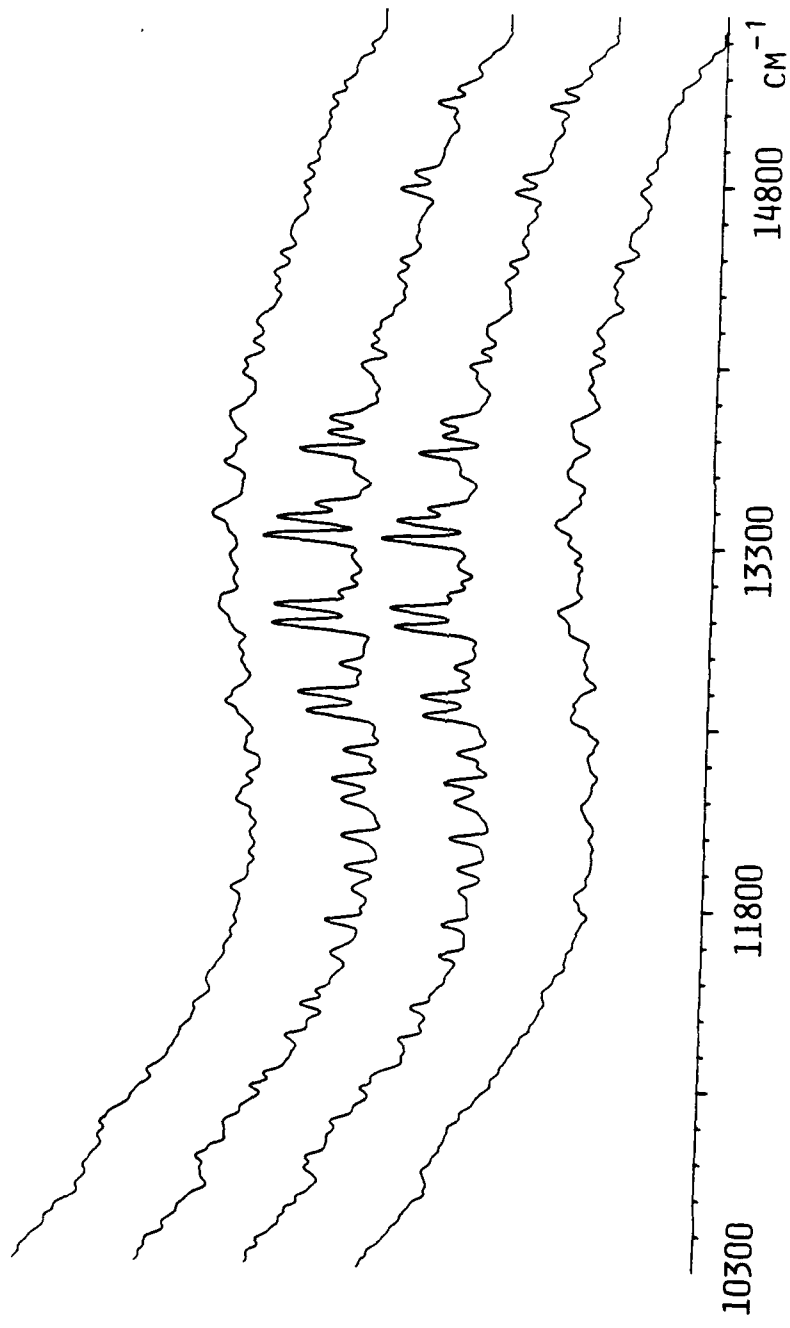


Fig. 2

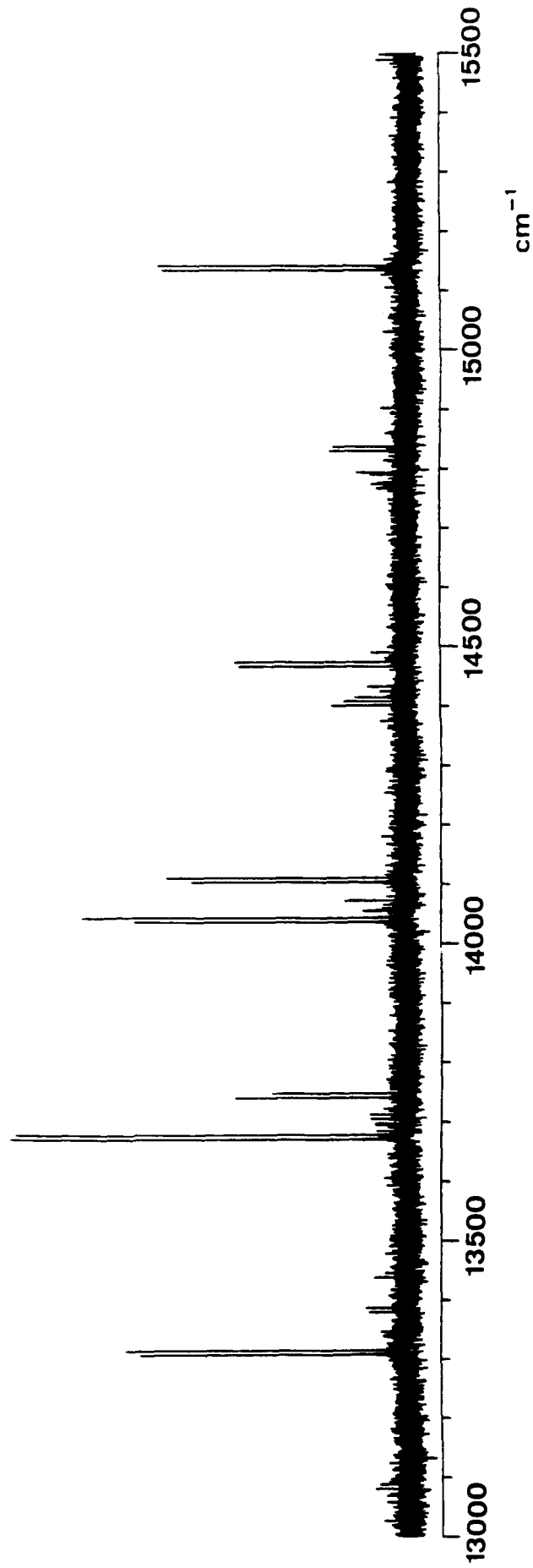
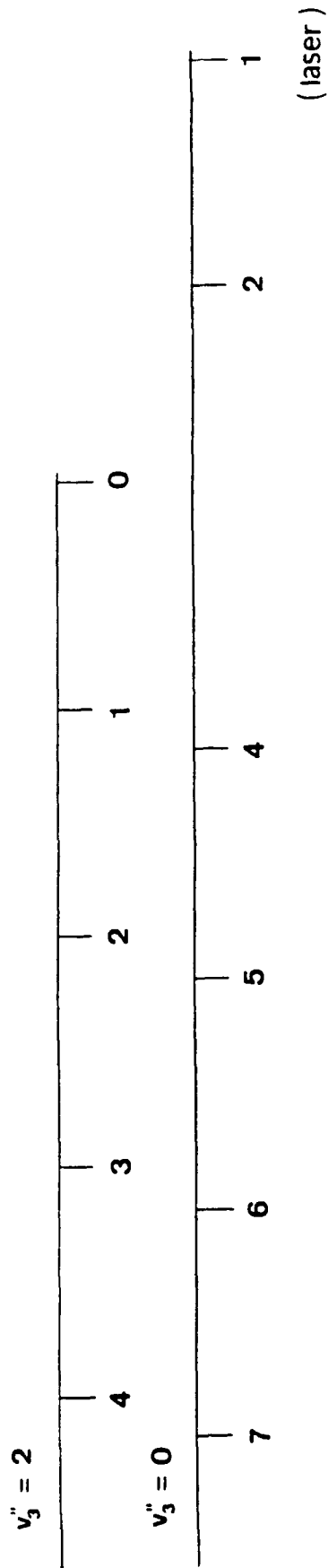
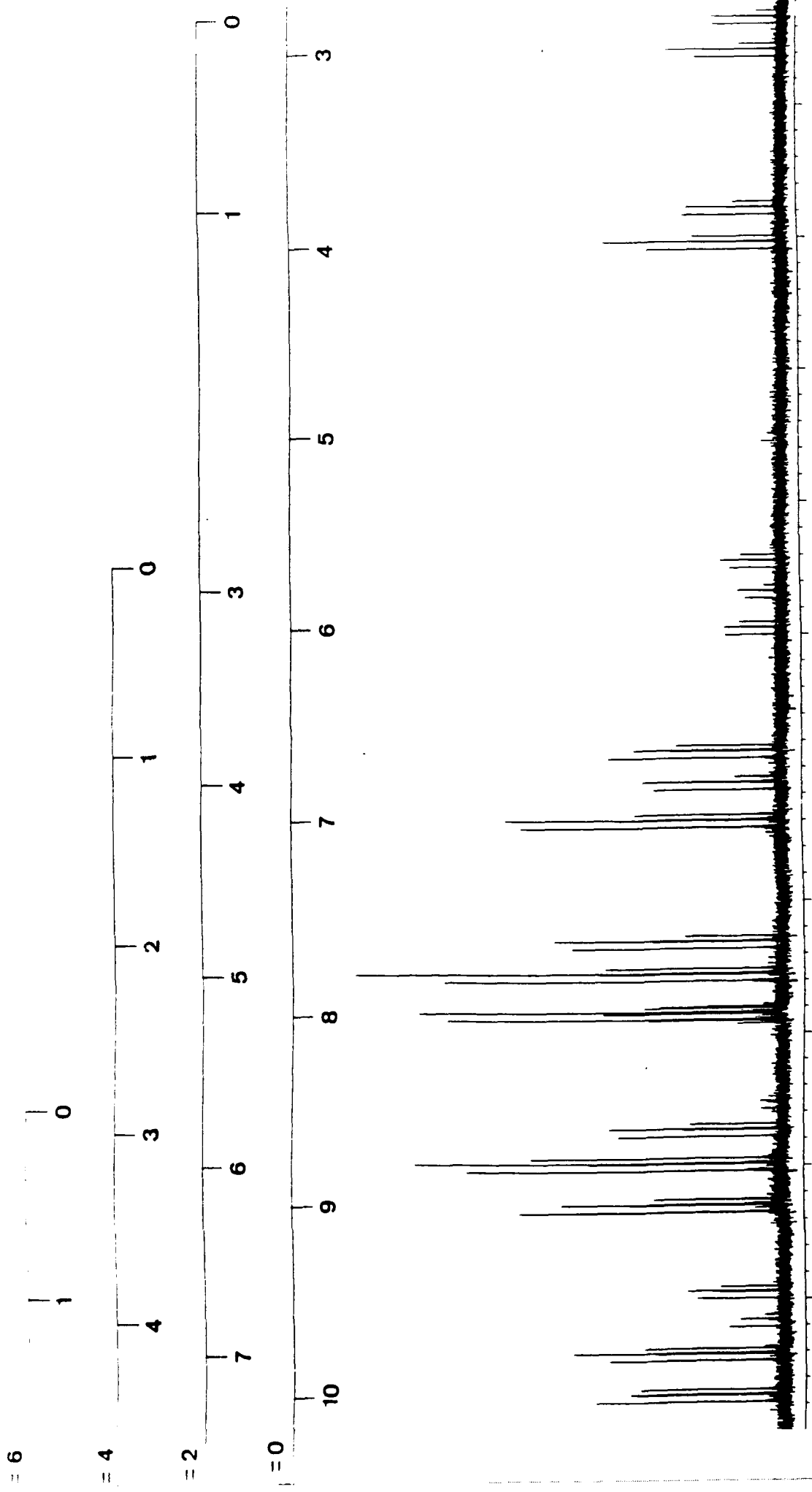


Fig. 3 a



cm⁻¹

14525

13525

12525

Fig. 36

Page 21

$v_1''=2$ $v_3''=4$

$v_1''=5$ $v_3''=2$

$v_1''=8$ $v_3''=0$

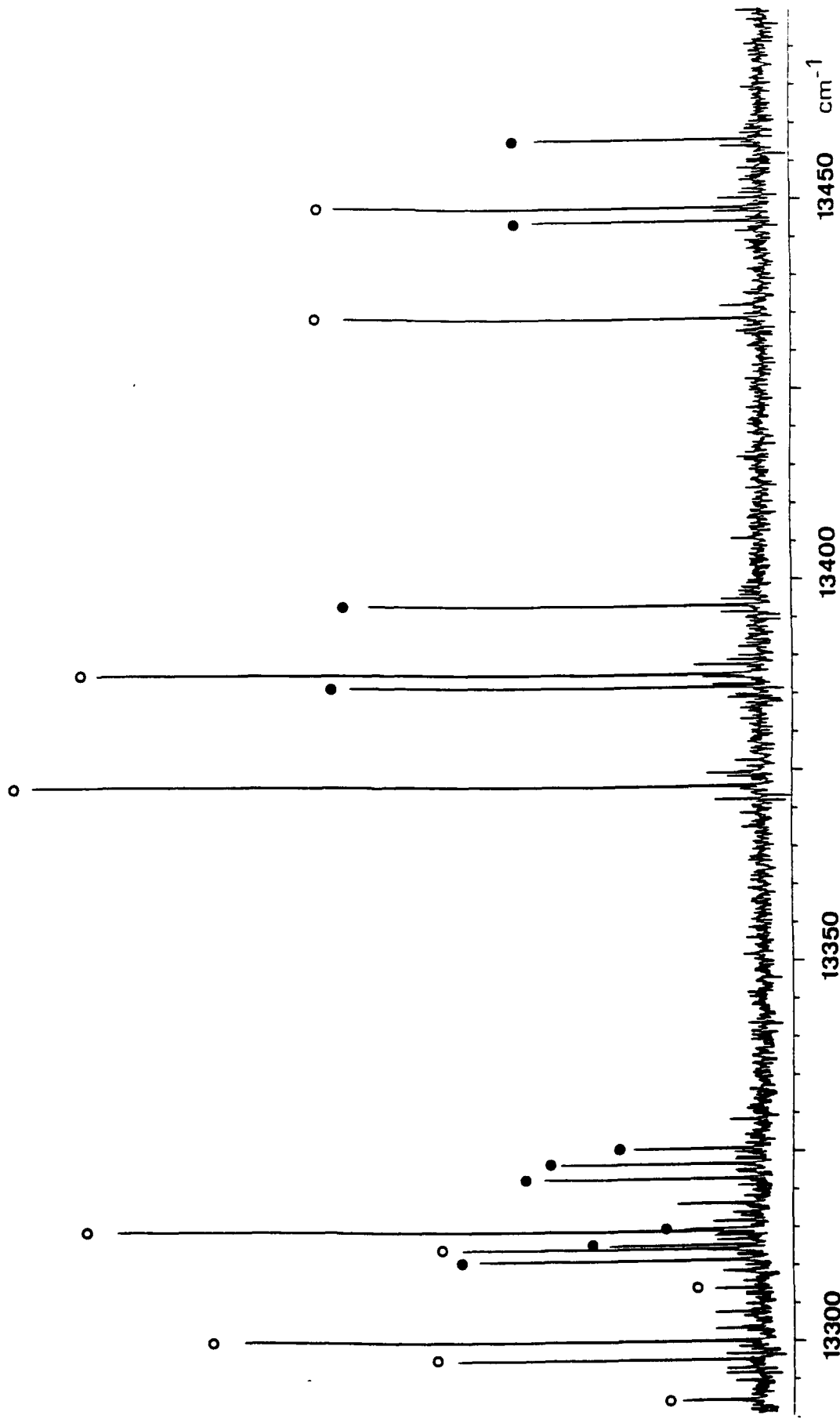


Fig. 4

APPENDIX 6

GCL'92 - 9th INTERNATIONAL SYMPOSIUM ON GAS FLOW AND CHEMICAL LASERS
21-25 September 1992 - HERAKLION, SPIE (To be published)

Chemiluminescence of the reaction of metastable oxygen with copper and comparison with the laser induced fluorescence of the CuCl₂ molecule

A.J. Bouvier¹, R. Bacis¹, S. Churassy¹, J.C. Coste¹, P. Crozet¹, B. Erba¹, J.B. Koffend²,
M. Lamrini¹, A.J. Ross¹ and I. Russier¹

¹ Laboratoire de Spectrométrie Ionique et Moléculaire, URA CNRS n°171, Université Lyon I,
43 Bd du 11 Novembre 1918, 69622 Villeurbanne Cedex, France

² The Aerospace Corporation, Box 92957, Los Angeles, California 9009, USA

ABSTRACT

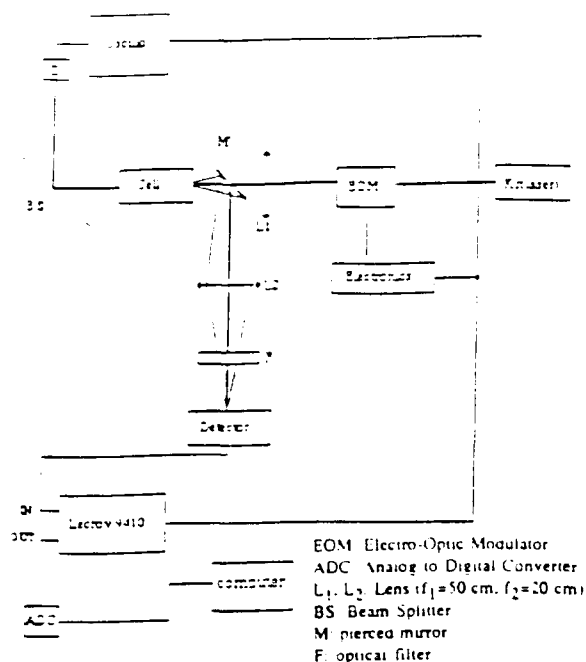
In order to better understand the strong chemiluminescence occurring during the chemical reaction between Cl₂, O₂(¹Δ_g) and Cu at 400°C, we have investigated the electronic states of CuCl₂, recording Fourier transform spectra and measuring lifetimes of the ²Π_u, ²Δ_g states. Implications on the likelihood of obtaining a chemical laser from this system are evoked.

1. INTRODUCTION

In 1989, Yoshida *et al*¹ published a report on an intense red and infrared chemiluminescence produced by flowing chemically generated metastable oxygen O₂(¹Δ_g) over a heated copper rod (200-400°C). Their claim to have observed laser oscillation at 703 nm in this chemical system^{1,2} motivated further investigations in the fields of spectroscopy and laser research, to identify and understand the species and processes involved. Several possible emitters were proposed.^{3,4,5,6} but the situation was clarified by the work of Zhuang *et al*³ and of Huang *et al*.⁶ who demonstrated that chlorine was essential to this process. This suggested that chlorine was doing more than reacting with hydrogen peroxide to produce singlet oxygen, as replacing Cl₂ with Br₂ produced metastable oxygen, but not the chemiluminescence. This observation fitted with the suggestion from Tokuda *et al*⁵ that CuCl₂ was responsible for the red and infrared emission, and that the copper dichloride was formed when surplus chlorine gas from the chemical generator of singlet oxygen made contact with the heated copper. We tested the hypothesis put forward by Tokuda *et al*.⁵ by comparing the emission from the chemical reaction between O₂(¹Δ_g), Cl₂ and heated copper, with spectra of CuCl₂.

2. EXPERIMENT

Broadly, our experimental work falls into two categories, Fourier transform (FT) spectroscopy and fluorescence lifetime measurements. Low (1 cm⁻¹) resolution spectra of the red and IR emission from the O₂(¹Δ_g) + Cl₂ + Cu reaction were recorded on a commercial FT spectrometer. This work has already been reported in detail.^{7,8} Absorption spectra and laser induced fluorescence (LIF) spectra of CuCl₂ were also recorded, at higher resolution. Using a tunable cw single mode laser and the FT spectrometer at a resolution = .07 cm⁻¹, we resolved rotational structure in the ²Π_u - ²Π_g transition of CuCl₂. Again, full details are given elsewhere.⁹ Recently we have used the 6471 Å line of a krypton ion laser — which excites the ²Π_u - ²Π_g transition in CuCl₂⁸ — and an electro-optic modulator to measure the decay of the red ²Π_u → ²Π_g fluorescence in CuCl₂, and of the weaker IR fluorescence around 1.2 μm which is attributed to the ²Δ_g → ²Π_g transition. The experiment arrangement is illustrated in Fig. 1.



The electro-optic modulator generated 1 kHz boxcar light pulses 700 μ s long, which excite the fluorescence in the CuCl_2 cell. Backwards fluorescence was collected and focused through an appropriate optical filter on to either a red (photomultiplier tube) or infrared (Ge) detector. The signal from the detector was transmitted to a digital oscilloscope (Lecroy 9410), where the fluorescence decay could be measured with respect to the reference signal from the electro-optic modulator. Data were stored on a personal computer. The auxiliary detection circuit, which detected a small part of the laser beam travelling through the cell, served to monitor the experiment in real time. The experiment was repeated at different vapour pressures of CuCl_2 in the cell. The time response of the system was = 50 ns using the photomultiplier, and = 1 μ s with the Ge detector.

Figure 1. Experimental set up for fluorescence decay.

3. RESULTS

3.1. Chemiluminescence and absorption experiments

For completeness, we show the Fourier transform spectra of the emission recorded during the chemical reaction between singlet oxygen, chlorine and heated copper (= 200°C) in Fig. 2. In Fig. 3, the infrared spectrum at higher resolution (trace a) is compared with the absorbance of CuCl_2 (trace c), and a typical laser induced (DCM) fluorescence spectrum of CuCl_2 (trace b) in the same region. The coincidence between the heads of the bands in these three spectra suggests (i) that CuCl_2 is responsible for the IR chemiluminescence, (ii) that the ground state of CuCl_2 is involved in the electronic transition, because the ground state is necessarily involved in the absorption experiment. From the ab initio calculations of Bauschlicher *et al.*¹⁰ the upper state in the IR system is likely to be ${}^2\Delta_g$.

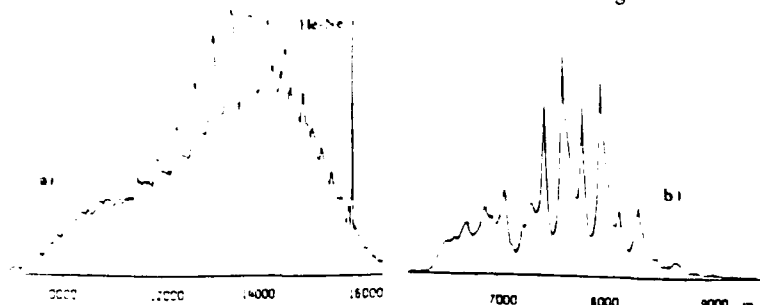


Figure 2. a) Chemiluminescence from the reaction $\text{Cu} + \text{Cl}_2 + \text{O}_2({}^1\Delta_g)$ at 350°C in the visible region. b) Chemiluminescence from the reaction $\text{Cu} + \text{Cl}_2 + \text{O}_2({}^1\Delta_g)$ at 350°C in the infrared.

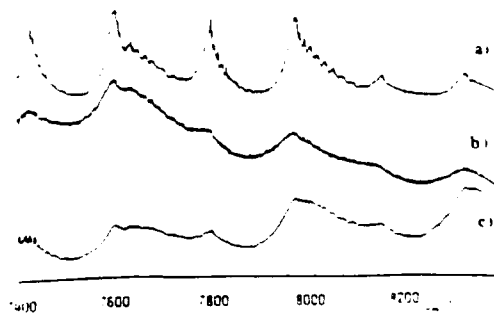


Figure 3. Infrared spectra recorded at 0.5 cm^{-1} resolution. a) Chemiluminescence from the reaction $\text{Cu} + \text{Cl}_2 + \text{O}_2({}^1\Delta_g)$ at 350°C. b) Laser induced fluorescence, after subtraction of the blackbody contribution from the oven. This spectrum was totally insensitive to the choice of the laser wavelength. c) The absorbance spectrum of CuCl_2 at 700°C (cell $l = 10$ cm).

3.2. cw Laser Induced Fluorescence (LIF) experiments in CuCl₂

The red FT spectra showed discrete fluorescence, containing very simple rotational line patterns occurring to a number of vibrational levels of the ground state (${}^2\Pi_g$) of CuCl₂, superposed on a broad continuum. Analysis of these spectra has been described elsewhere⁹ for the most common species present (${}^{63}\text{Cu}{}^{35}\text{Cl}_2$), but we have now extended this to cover ${}^{65}\text{Cu}{}^{35}\text{Cl}_2$, ${}^{63}\text{Cu}{}^{35}\text{Cl}{}^{37}\text{Cl}$ and ${}^{65}\text{Cu}{}^{35}\text{Cl}{}^{37}\text{Cl}$. We have identified the vibrational structure as combinations of the symmetric stretch, ν_1 with even quanta of ν_3 , the antisymmetric stretch. From a linear least squares fit, we have derived constants for three unassigned levels of the upper (${}^2\Pi_u$) state in the form of effective term energies, rotational and distortion constants, and we have a polynomial expression for the lower state, which contains effective equilibrium constants for the symmetric and antisymmetric stretches (ω_1, ω_3), anharmonicity terms, and rotational terms. Numerical values are given in Tables 1 and 2.

Table 1. Constants for the ${}^2\Pi_u$ state (cm^{-1}).

	${}^{63}\text{Cu}{}^{35}\text{Cl}_2$	${}^{63}\text{Cu}{}^{35}\text{Cl}{}^{37}\text{Cl}$
$\nu = 0$	$T = 15546.179$ $B' = 0.05194$ $D' = 8.37 \cdot 10^{-9}$	15548.151 0.0506 $8.40 \cdot 10^{-9}$
$\nu = 1$	$T = 15882.155$ $B' = 0.051764$ $D' = 8.41 \cdot 10^{-9}$	15880.352 0.0505 $8.40 \cdot 10^{-9}$
$\nu = 2$	$T = 16257.092$ $B' = 0.051330$ $D' = 8.45 \cdot 10^{-9}$	16252.531 0.0498 $8.40 \cdot 10^{-9}$

T with respect to the lowest level of ${}^2\Pi_g$

Table 2. Constants for the ${}^2\Pi_g$ state (cm^{-1}).

	${}^{63}\text{Cu}{}^{35}\text{Cl}_2$	${}^{65}\text{Cu}{}^{35}\text{Cl}_2$	${}^{63}\text{Cu}{}^{35}\text{Cl}{}^{37}\text{Cl}$	${}^{65}\text{Cu}{}^{35}\text{Cl}{}^{37}\text{Cl}$
ω_1	371.9	371.9	366.6	366.4
ω_3	525.5	521.1	522.8	518.3
X_{11}	-0.53	-0.53	-0.50	-0.49
X_{33}	-1.11	-1.06	-1.20	-1.17
X_{13}	-2.57	-2.56	-2.54	-2.46
B_e	0.05828	0.05828	0.05658	0.05659
α_1	$1.25 \cdot 10^{-4}$	$1.21 \cdot 10^{-4}$	$1.0 \cdot 10^{-4}$	$1.4 \cdot 10^{-4}$
α_3	$1.95 \cdot 10^{-4}$	$1.8 \cdot 10^{-4}$	$2.0 \cdot 10^{-4}$	$1.7 \cdot 10^{-4}$
D_e	$0.9 \cdot 10^{-8}$	not determined	$1.9 \cdot 10^{-8}$	$0.7 \cdot 10^{-8}$

An individual laser induced fluorescence spectrum bears little resemblance to the red flame, which is not surprising because ideally the LIF spectrum should — and does — contain very little rotational information. Summing several LIF results, we find a more encouraging comparison, as several isotopic species start to appear, and the rotational levels are better represented. Using preliminary constants of Tables 1 and 2, and intensity data from the LIF work (derived from the discrete part of the LIF spectra), it is possible to calculate a theoretical ${}^2\Pi_u - {}^2\Pi_g$ spectrum. The red flame, summed LIF spectra and simulated spectrum are shown in Fig. 4.

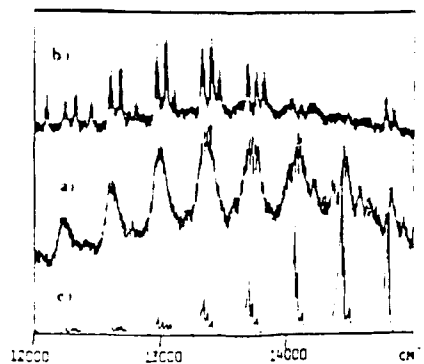


Figure 4. a) Chemiluminescence of $\text{Cu} + \text{Cl}_2 + \text{O}_2({}^1\Delta_g)$. b) Sum of several fluorescence spectra of CuCl₂ (laser = 607 nm). c) Yoshida flame simulation using calculated spectroscopic constants of the four main isotopomers of CuCl₂.

3.3. Lifetime measurements

The fluorescence decay was measured at a series of different vapour pressures of CuCl_2 (controlled by varying the temperature of the sidearm on our sealed quartz cell). Extrapolating to low pressures, we derived radiative lifetimes for the excited states of CuCl_2 as: $\tau_{\text{red}} \leq 70$ ns for the $^2\Pi_u$ state, $\tau_{\text{IR}} = 3.0 \pm 0.8$ μs for the $^2\Delta_g$ state. We also measured the rise time for the IR signal to be 2.9 ± 0.6 μs which is significantly slower than the response of the detection system, and which — curiously — matches the IR fluorescence decay. It thus seems that the IR signal is generated by a collisional mechanism, as has been discussed in ref. 7. The disparity between radiative lifetimes of the $^2\Pi_u$ and $^2\Delta_g$ states confirms that the red $^2\Pi_u - ^2\Pi_g$ transition is allowed, whilst the IR $^2\Delta_g - ^2\Pi_g$ transition is electronically forbidden.^{8,10} The $^2\Delta_g$ state is thus metastable, and therefore might be able to sustain a population inversion. Laser action in the red seems unlikely, with $\tau(^2\Pi_u) \leq 70$ ns, and our attempts to produce an optically pumped CuCl_2 laser at 700 nm have failed.

4. CONCLUSION

Spectral similarities between the infrared chemiluminescence observed during the reaction of $\text{O}_2(^1\Delta_g) + \text{Cl}_2 +$ heated copper and absorption or LIF spectra of copper dichloride suggest that CuCl_2 carries the IR emission first reported by Yoshida *et al.*^{1,2} Equally, a comparison between the red chemiluminescence of this system and results from laser induced fluorescence spectroscopy tend to confirm this. Lifetime measurements made on the red and IR systems of CuCl_2 match theoretical assignments of the electronic states of CuCl_2 ,¹⁰ and fit also with the differences in intensity between the red (strong) and IR (weak) systems reported by Yoshida.

The question of using this chemical system as a laser was one of the main motivations for this study. Lifetime measurements in the red system of CuCl_2 make this most unlikely at 700 nm, but the metastable $^2\Delta_g$ state could reasonably be expected to sustain a population inversion with respect to the ground state of CuCl_2 provided that the population of this electronic state of CuCl_2 (e.g. by collision with $\text{O}_2(^1\Delta_g)$) remains highly efficient.

It seems clear that metastable oxygen is well suited to excite the $^2\Delta_g - ^2\Pi_g$ transition in CuCl_2 (near resonance in energy), but we believe that the metastable oxygen may also be involved in energy transfer at an earlier stage, because our simple chemical reaction, $\text{Cu} + \text{Cl}_2 \rightarrow \text{CuCl}_2$ at 200–400°C would not normally produce an appreciable concentration of CuCl_2 in the gas phase in our experimental conditions.

Acknowledgements: This work benefited from financial support from the Air Force Office of Scientific Research (grant AFOSR-91-0235) and from the Direction des Recherches, Etudes et Techniques (grant 901609/A000/DRET/DS/SR).

5. REFERENCES

1. S. Yoshida, M. Taniwaki, T. Sawano, K. Shimizu and T. Fujioka, *Jpn J. Appl. Phys.*, vol. 28, p. L-381, 1989.
2. S. Yoshida, K. Shimizu, T. Sawano, T. Tokuda and T. Fujioka, *Appl. Phys. Lett.*, vol. 54, p. 2400, 1989.
3. Q. Zhuang, J. J. Kui, F.T. Sang, Q.N. Yuan, R.Y. Zhang, H.P. Yang, Li Li Q.S. Zhu and C.H. Zhang, Conference Proceedings 8th International Symposium on Gas Flow and Chemical Lasers, Madrid, Spain, 1990.
4. R. Bacis, J. Bonnet, A.J. Bouvier, S. Churassy, P. Crozet, B. Erba, E. Georges, J. Lamarre, Y. Louvet, M. Nota, D. Pigache, A.J. Ross and M. Setra, *Europh. Lett.*, vol. 12, p. 569, 1990.
5. T. Tokuda, N. Fujii, S. Yoshida, K. Shimizu and I. Tanaka, *Chem. Phys. Lett.*, vol. 174, p. 385, 1990.
6. R. Huang, R. Zhang and R.N. Zare, *Chem. Phys. Lett.*, vol. 170, p. 437, 1990.
7. A.J. Bouvier, R. Bacis, J. Bonnet, S. Churassy, P. Crozet, B. Erba, J.B. Koffend, J. Lamarre, M. Lamrini, D. Pigache and A.J. Ross, *J. Physique IV*, vol. 1, p. 663, 1991.
8. A.J. Bouvier, R. Bacis, J. Bonnet, S. Churassy, P. Crozet, B. Erba, J.B. Koffend, J. Lamarre, M. Lamrini, D. Pigache and A.J. Ross, *Chem. Phys. Lett.*, vol. 184, p. 133, 1991.
9. A.J. Ross, R. Bacis, A.J. Bouvier, S. Churassy, J.C. Coste, P. Crozet and I. Russier, *J. Mol. Spectrosc.* (accepted).
10. C.W. Bauschlicher, and B.O. Roos, *J. Chem. Phys.*, vol. 91, p. 4785, 1989.